TECHNISCHE UNIVERSITÄT DRESDEN

JOINT PROJECT

INTERACTION AND TRANSPORT OF ACTINIDES IN NATURAL CLAY ROCK WITH CONSIDERATION OF HUMIC SUBSTANCES AND CLAY ORGANICS

Subproject

Investigations of temperature dependence of complexation und sorption of trivalent actinides (Am(III)) in the system actinid-NOM-natural clay rock-aquifer

MARGRET ACKER, ASTRID BARKLEIT, MELANIE MÜLLER, JULIANE SCHOTT, GERT BERNHARD

FINAL REPORT

TU Dresden
Sachgebiet Strahlenschutz
Professur für Radiochemie
01062 Dresden
http://tu-dresden.de

Das diesem Bericht zugrunde liegende Vorhaben wurde mit Mitteln des Bundesministeriums für Wirtschaft und Technologie unter dem Förderkennzeichen **02 E 10417** gefördert.
Die Verantwortung für den Inhalt dieser Veröffentlichung liegt bei den Autoren.

VERBUNDVORHABEN: Wechselwirkung und Transport von Actiniden im natürlichen Tongestein unter Berücksichtigung von Huminstoffen und Tonorganika

TEILPROJEKT: Untersuchungen zur Temperaturabhängigkeit der Komplexbildung und Sorption dreiwertiger Actinide (Am(III), Pu(III)) im System Actinid-NOM-natürliches Tongestein-Aquifer

Ausführende Institution:

TU Dresden
Fakultät für Mathematik und Naturwissenschaften
Fachbereich Chemie und Lebensmittelchemie
Professur für Radiochemie
01062 Dresden

TU Dresden
Sachgebiet Strahlenschutz
01062 Dresden

Dresden, den 06.12.2011

Abstract

The main objective of this project was to study the interaction processes between An(III)/Ln(III) (represented by Am(III) and Eu(III), respectively), organic model ligands, and Opalinus Clay at elevated temperature (until 80°C). The thermodynamic data (logβ, ΔG, ΔH and ΔS) for the complexation and sorption processes have been obtained. This broadens the thermodynamic database by data at elevated temperatures.

The complexation of Am(III)/Eu(III) with small organic ligands (pyromellitic, salicylic, lactic, acetic, citric, and tartaric acid) that serve as model ligands for natural organic material, like humic substances or clay organic was investigated by temperature dependent UV-vis and time-resolved laser-induced fluorescence spectroscopy (TRLFS).
For the first time, the UV-vis absorption spectroscopy utilizing an Long Path Flow Cell (LPFC) has been established for the speciation analysis of Am(III) at trace concentrations. A detection limit of $5 \cdot 10^{-9}$ mol·L^{-1} Am(III) was determined with a 2 m LPFC.
Several Am(III)/Eu(III)-organic ligand complexes were spectroscopically and thermodynamically characterized. General, all studied complexation reactions are endothermic and driven by entropy.
Furthermore, the interaction of Eu(III) with pyromellitc acid (1,2,4,5-benzene-tetracarboxylic acid) had been studied in detail with additional methods like isothermal titration calorimetry (ITC) and Fourier-transform infrared spectroscopy in combination with density function theory (DFT) calculations. At elevated temperature and higher concentration (> 5 mM Eu(III) and pyromellitic acid) a temperature-dependent polymerization was observed. It had been shown, that predominantly chelating coordination with two carboxylic groups in the monomeric complex and monodentate binding of a single carboxylic group in the polymeric complex of the polycarboxylate with Eu(III) occur.

The sorption of Eu(III) on Opalinus Clay was investigated in absence and presence of the small organic ligands citric and tartaric acid at different temperatures and under synthetic pore water conditions (I = 0.4 M, pH = 7.6) by batch experiments. Time-resolved laser-induced fluorescence spectroscopy was used for analysis of the Eu(III) speciation in the binary system Eu(III)-Opalinus clay and ternary system Eu(III)-Opalinus clay-small organic ligand under pore water conditions.
The Eu(III) sorption was found to increase generally with temperature in a considerably endothermic reaction with an enthalpy of about 50 kJ·mol^{-1}. In presence of tartrate or citrate the Eu(III) sorption decreases with increasing ligand concentration due to a complex formation of Eu(III) in solution. This complex formation was verified by TRLFS investigations. The detected Eu(III) surface species on Opalinus Clay with a luminescence lifetime of (201 ± 9) µs is no influenced by the presence of the studied organic ligands.

Contents

1 Introduction 1

2 Am(III) and Eu(III) complexation by small organic ligands 3

2.1 Experimental 3

2.2.1 Solutions and reagents 3

2.1.2 Potentiometric titrations 3

2.1.3 Time-resolved laser-induced fluorescence spectroscopy 3

2.1.4 UV-vis spectroscopy with a Long Path Flow Cell 5

2.1.5 Data analysis and determination of complex formation constant 8

2.1.6 Fourier-transform infrared (FTIR) spectroscopy and Density functional theory (DFT) calculation 9

2.1.7 Isothermal titration calorimetry 9

2.2 Results and discussions 10

2.2.1 Potentiometric titration 10

2.2.2 Pyromellitic acid 11

2.2.3 Salicylic acid 20

2.2.4 Lactic acid 22

2.2.5 Citric, tartaric, and acetic acid 25

2.3 Conclusions and update of the thermodynamic database 28

3 Eu(III) sorption on Opalinus Clay. 31

3.1 Experimental 31

3.1.1 Solutions and reagents 31

3.1.2 Batch experiments 31

3.1.3 Time-resolved laser-induced fluorescence spectroscopy 32

3.2 Results and discussion 33

3.2.1 Influence of Eu(III) concentration 33

3.2.2 Influence of pH 34

3.2.3 Influence of temperature 37

3.2.4 Influence of small organic ligands 40

3.3 Conclusions 43

4 References 44

1 Introduction

To assess the long-term safety of nuclear waste repositories for high level radioactive waste a wide knowledge about the chemical and physical behaviour of radionuclides, particularly the actinides, is essential. In worst case scenarios like a water inleakage into the repository a multitude of reactions of the stored radionuclides with solved or suspended components as well as interactions with the host rocks and backfill materials have to be considered quantitatively.
At present, argillaceous rock, like the Opalinus Clay formation in Switzerland, are under examination as potential host rocks for nuclear waste repositories due to their high sorption capacity for radionuclides, water impermeability and swelling properties [HOT2007, NAG2002]. In the framework of our project "Interaction and transport of actinides in natural clay rock with consideration of humic substances and clay organic" Opalinus Clay (OPA sample from bore core BHE-24/1) was chosen as model for such natural argillaceous rock. Opalinus clay consists of clay minerals like illite, chlorite, and kaolinite as well as minerals like quartz, calcite, pyrite, and siderite as main components [NAG2002]. In a repository based on argillaceous rock an initial temperature of around 100°C is expected [NAG2002] and should not be exceeded during the storage of radioactive waste [NEL2008]. The risk assessment has to consider this temperature, since the individual processes that determine the migration behaviour of radionuclides in a repository depend significantly on the temperature.
Opalinus clay contains natural organic matter up to 1 %. Such natural organic matter (NOM) includes large macromolecules, like the ubiquitous humic and fulvic substances, kerogene as well as small molecules, like acetate or lactate, which are well soluble in water [HOT2007]. These compounds can interact as complexing agents with radionuclides and therefore impact the radionuclide migration. Thus, reliable thermodynamic data for the complexation behaviour of radionuclides with NOM are crucial to model and to predict the radionuclide transport in the near and far field of a nuclear waste repository.

The current thermodynamic databases are lacking fundamental data for the complexation of trivalent americium with small ligands at elevated temperatures. These small organic ligands like pyromellitate, salicylate, acetate, citrate, lactate, and tartrate can serve as model ligands for NOM. One aim of the project was to study the complexation behaviour of Am(III) and Eu(III) with these small organic ligands at higher temperature, up to 60°C. From the temperature dependent complexation constants the complexation enthalpies and entropies can be derived.

Two different spectroscopic methods were applied to study the compexation behaviour in detail. The time-resolved laser-induced fluorescence spectroscopy (TRLFS) was carried out to study the Eu(III) and for the first time also the Am(III) complexation with small molecule ligands. The UV-vis spectroscopy with an Long Path Flow Cell was applied to study the Am(III) complexation reactions at low Am(III) concentrations ($< 5 \cdot 10^{-7}$ M) which are of higher relevance for environmental conditions than the typically concentration of about $\sim 1 \cdot 10^{-4}$ M used in UV-vis measurements with a 1 cm cuvette. Additional the isothermal microtitration calorimetry (ITC) as well as FT-IR measurements in combination with DFT calculations were used to investigate the Eu(III) complexation with pyromellitic acid in detail.

So far, investigations on the retention behaviour of OPA to radionuclides are mainly limited to ambient temperature [HAR2008, FRÖ20011, GLA2005, JOS2011, WU2009]. Only few studies deal with the impact of temperature on the radionuclide retention [BAU2005, TER2005, TER2006]. Tetre et al. [TER2006] investigated the sorption of different lanthanides on montmorillonite up to 150°C and observed that the sorption increases with

rising temperature at pH > 6. Bauer et al. did not observe any impact of temperature [BAU2005]. These contradictory results concerning the influence of temperature gave rise to the second aim of the present work to investigate the sorption of Eu(III) at elevated temperatures up to 60°C.

As a third aim, the impact of the small organic ligands on the Eu(III) sorption at elevated temperatures was studied. In literature was found that organic and inorganic ligands either increase or decrease the sorption of radionuclides (in dependence of pH, ionic strength, the concentration of complexing agents, the nature of complexing agents, and of the sorbent). Pathak et al. [PAT2007] found an increase of the Eu(III) sorption on silica in the presence of oxalate and phosphate due to the formation of ternary surface complexes, and a decrease of the Eu(III) sorption in the presence of acetate, carbonate, citrate, and EDTA due to a complex formation in solution in sequence of the complex formation strength of these ligands (acetate < carbonate < citrate < EDTA). In this work two small organic ligands, the citric and the tartaric acid were chosen as model ligands.

The present work discusses the Eu(III) sorption on OPA under realistic OPA pore water conditions (pH 7.6, I = 0.4 M). The temperature influence and the impact of tartaric and citric acid on the Eu(III) sorption on OPA was investigated by batch sorption experiments up to 60°C. The temperature dependent distribution coefficients R_d were determined and the thermodynamic parameters enthalpy and entropy of the sorption were derived. In addition TRLFS investigations and experiments with ^{14}C-labeled citric acid provided an insight into the sorption mechanism and the influence of the organic ligands.

This work was part of a BMWi joint project between the Universities Mainz, Potsdam, München, Saarbrücken and the Institute of Nuclear Waste Management at the Karlsruher Institute of Technology and the Institute of Radiochemistry at the Helmholtz-Zentrum Dresden-Rossendorf.

2 Am(III) and Eu(III) complexation by small organic ligands

2.1 Experimental

2.1.1 Solutions and reagents

Eu_2O_3, $EuCl_3 \times 6H_2O$, pyromellitic acid, salicylic acid, sodium salicylate, tartaric acid and sodium lactate were purchased from Aldrich or Fluka and used without further purification. Eu_2O_3 was dissolved in 0.1 M $HClO_4$ to obtain a $5 \cdot 10^{-3}$ M Eu(III) stock solution. The Eu(III) concentration was verified with ICP-MS (Perkin Elmer).
The ^{243}Am(III) stock solution was prepared by dissolving of AmO_2 powder (Oak Ridge National Laboratory) in 30% HNO_3. The Am(III) concentrations of sample solutions as well as the purity of the isotope was verified by α- and γ-spectrometry (Canberra, Ortec). Only the daughter nuclide of α-decay, Np-239 (half-life: 2.355 d), in equilibrium was determined (about 0.0001 % of Am).
In the complexation experiments, the ionic strength was adjusted with $NaClO_4$ (Merck, analytical grade) to 0.1 M. Necessary pH adjustments were performed with a pH meter (WTW) consisting of a pH electrode (Blue Line, Schott), filled with 3 M KCl, and a temperature sensor. The pH electrode was calibrated with buffer solutions (Merck) at the selected temperature. The adjustments were carried out with small amounts of NaOH (Merck) and $HClO_4$ (Merck) solutions of different concentrations with an accuracy of 0.05 pH units.

2.1.2 Potentiometric titration

Samples were prepared in an inert gas box (nitrogen) with carbonate-free deionized water. The measurements were carried out at CO_2 free condition under nitrogen atmosphere in 0.1 M $NaClO_4$ as an acid-base titration. 30 mL samples of 0.01 M ligand (pyromellitic acid, salicylic acid, tartaric acid, initial pH 2.0 each) were automatically titrated (736 GP Titrino / TiNet 2.50, Metrohm) with 0.1 M NaOH (carbonate-free, Titrisol, Merck) at temperatures between 10 and 60°C. Dynamic titration was used with a minimum drift of 0.5 mV/min and a delay time of at least 60 s at each point before measuring the pH with a Schott BlueLine 11 pH combination electrode with platinum diaphragm. The electrode was calibrated for each experimental run with standard buffers (pH 4.008 and 6.865, Schott). Titrations were done in triplicate between pH 2 and 7 at each temperature and analyzed using the program HYPERQUAD2006.

2.1.3 Time-resolved laser-induced fluorescence spectroscopy

Europium
Luminescence spectra were recorded using a pulsed flash lamp pumped Nd:YAG-OPO laser system from Continuum (Santa Clara, CA, U.S.A.) as described in [MOL2008]. The excitation wavelength was 394-395 nm. A constant time window of 1 ms was used for all measurements. Static and time-dependent luminescence spectra of Eu(III) were recorded at 565 – 650 nm (1200 line mm^{-1} grating, 0.2 nm resolution, 2000 accumulations) and at 440 – 780 nm (300 line mm^{-1} grating, 0.7 nm resolution, 200 accumulations), respectively. For time-resolved measurements, 41 spectra were recorded with 15-50 µs separation. Spectrophotometric titrations were done at least in triplicate starting with 5, 10 or 30 µM Eu(III) in 0.1 M $NaClO_4$ at pH 5.0 or 6.0. Subsequent additions of aliquots of a 0.01, 0.1, 0.5 or 2.5 M ligand stock solution (0.1 M $NaClO_4$, pH 5.0 or 6.0) covered ligand concentrations

from 10.0 µM to 1 mM (pyromellitic acid) or 0.1 M (salicylate, lactate). At least 20 spectra each were measured in the 25 to 70°C range using a stirred temperature-controlled cuvette holder (Flash 300TM, Quantum Northwest, U.S.A.) and 30 min initial equilibration time and additional 10 min after each injection of ligand at a given temperature.

Americium

For the first time Am(III) complexation with a small organic ligand was characterized with time-resolved laser-induced fluorescence spectroscopy (TRLFS) at room temperature and trace metal concentration [BAR2011a]. Only few speciation studies of Am(III) have been published until now, using the emission of the $^5D_1$-$^7F_1$ transition at around 690 nm [BEI1994, KIM1998, KIM2001, RUN2000, STU2006, THO1993, YUS1990].

For spectrophotometric TRLFS titration 2.7 mL of 2 µM Am^{3+} at pH 5.0 or 6.0 and 0.1 M $NaClO_4$ were titrated with aliquots (3, 10 or 15 µL) of a 0.01, 0.1 or 1 M ligand solution (pH 5.0 or 6.0, 0.1 M $NaClO_4$). 10-20 titration steps up to a ligand concentration of 0.1 mM (pyromellitate) or 0.1 M (lactate) were performed; every mixture was allowed to equilibrate for at least 15 min. At the beginning and after every titration step both a static and a time-resolved fluorescence spectrum was measured for pyromellitic acid at room temperature and for lactic acid in a temperature range between 25 and 65°C using a stirred temperature-controlled cuvette holder (Flash 300TM, Quantum Northwest, U.S.A.).

The TRLFS measurements were carried out with a pulsed Nd:YAG-MOPO laser system from Spectra Physics (Mountain View, USA), combined with a Spectrograph M270 and an ICCD camera system Spectrum One from Horiba-Jobin Yvon. The time difference between the trigger of the laser system and the start of the camera was adjusted by a delay generator DG 540 from Stanford Research Instruments. The laser source was set to an excitation wavelength of 503-506 nm ($^7F_0$-$^5L_6$ transition) with pulse energies of 15 mJ. The optimum of excitation wavelength strongly depends on the absorption of the Am^{3+} ion which is red-shifting upon complexation. Fig. 2-1 shows the fluorescence intensity of the Am^{3+}(aq) ion (left) and Am^{3+} with 0.1 M lactate in dependency of the excitation wavelength. Whereas for the aquo ion 503-504 nm excitation causes the highest fluorescence intensity, for the Am-lac complex 506- 507 nm excitation is the best.

Emission spectra were recorded between 625 and 773 nm, averaging five spectra with accumulating total 2500 laser pulses. The gate time of the camera was set to be 1 µs. The step width between two spectra in time-revolved mode was 2 or 5 ns, 15-20 delay steps were measured for every sample. The spectrograph and the camera system were controlled by Spectramax from Horiba-Jobin Yvon.

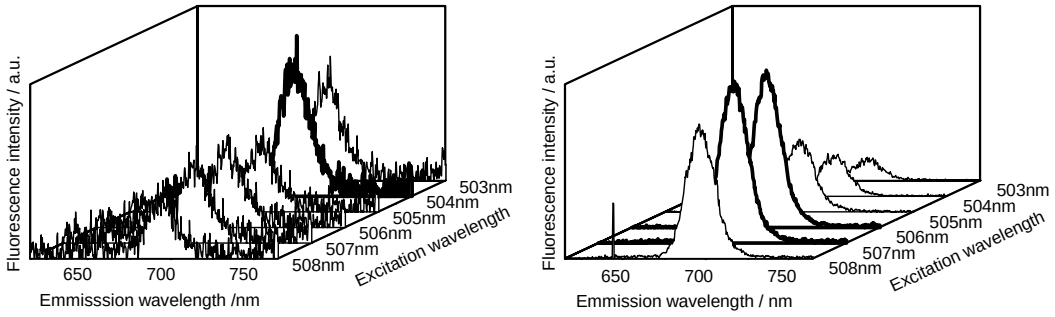

Fig. 2-1: Left: Emission spectra of 5 µM Am(III). Right: Emission spectra of 5 µM Am(III) and 0.1 M lactate in dependence of the excitation wavelength

Data analysis of the TRLFS spectra

TRLFS spectra were analyzed with Origin 7.5G to obtain the positions of peak maxima. Eu(III) spectra were normalized to the peak area of the $^5D_0$-$^7F_1$ transition. This magnetic dipole transition is independent from the chemical environment of the metal ion.

The luminescence lifetimes were determined from the time-resolved measurements with Origin by fitting the integrated luminescence signal of the emission bands to a sum of exponential decay functions:

$$E(t) = \sum_i E_i \cdot \exp(-t/\tau_i) \qquad (2\text{-}1)$$

E is the total fluorescence intensity at the time t, E_i the fluorescence intensity of the species i at the time t, and τ_i the corresponding lifetime.

With these lifetimes the number of water molecules was calculated using the following empirical equations [HOR1979, KIM1994b, and KIM1998]:

$$n(H_2O) \pm 0.5 = 1.07 \times \tau^{-1}\,(\text{ms}) - 0.62 \qquad \text{for Eu(III)} \qquad (2\text{-}2)$$

$$n(H_2O) \pm 0.5 = 2.56 \times 10^{-7} \times \tau^{-1}\,(\text{s}) - 1.43 \qquad \text{for Am(III)} \qquad (2\text{-}3)$$

2.1.4 UV-vis spectroscopy with a Long Path Flow Cell [MÜL2010]

TRLFS, see chapter 2.1.3, which is so far the most sensitive technique for measurements of actinide speciation, is limited to analytes that exhibit suitable fluorescence properties. In case of Am(III), the quantum yield of the fluorescence signal strongly depends on the solvent. In general, the nonradiative decay processes are predominant in aqueous solution [THO1993]. In sodium perchlorate medium the quantum yield of Am(III) is very low and the fluorescence emission lifetime very short (~ 23 ns, see chapter 2.2.2) in comparison to U(VI) or Cm(III), so that the detection limit of the used laser spectroscopic system described in chapter 2.1.3 is achieved. Therefore the UV-vis spectroscopy using a Long Path Flow Cell (**LPFC**, World Precision Instruments) for measurements of Am(III) speciation and non fluorescent actinides (for example Pu(III)) was established. A LPFC increases significantly the optical path of light through an analyte solution and therefore pushes detection limit towards lower concentrations according to Lambert Beer`s law [WAT1997, WIL2005].

A LPFC is a capillary cell made of silica tubing coated with Teflon AF, (an amorphous copolymere of tetrafluoroethylene and 2,2-bis(trifluoromethyl)-4,5-difluoro-1,3- dioxole) [MIC2003]. This material combines the properties of amorphous plastics with those of perfluorinated polymers and exhibits a high thermal and chemical stability, a good optical transparency, a low dielectric constant and the lowest refractive index for an organic polymer [RES1997]. The light propagates through the capillary by total internal reflection at the interface between silica and Teflon AF. LPFCs are available in different lengths from 0.05 to 5 m. The inner diameter of the capillary is only 500 to 550µm, thus a quite small sample volume is sufficient to fill the cell, which is an important fact for the work with radioactive actinides. The absorption spectroscopy utilizing a LPFC exhibits some specific features, for example the low spectral resolution of the mostly used fiber-optic spectrometer in support of a high signal to noise ratio, the great inner surface, which may cause wall adsorption and the light loss through the optical way and disturbing effects (like scattering by microparticles and gas bubbles, Schlieren formation) [INF2008].

The range for application of a 2 m LPFC is between 350 and 900 nm and with maximum transmission efficiency between 450 and 600 nm. The absorption spectra of Am(III) as well as of Eu(III) and Nd(III) exhibit prominent bands in this suitable wavelength range (Tab. 2-1). In our system the LPFC is coupled with a multichannel diode array spectrometer (MCS601, Carl Zeiss, spectral resolution < 2.3 nm) as detection system.
The determination complex stabilities at trace metal concentrations by UV-vis spectroscopy using a LPFC requires the characterization of the lower end of the measuring range of this system. The German Standard DIN 32645 [DIN08] provides two different types of decision limits for this purpose, depending on the analytical question which has to be answered. DIN 32645 [DIN08] is made for chemical analysis and describes the mathematical procedure for the evaluation of detection limit (DL) and for the limit of determination (LoD). Both are critical values of the measured variable. The detection limit is adequate to answer the question whether the analyte is present or not. The limit of determination (DoL) describes the lowest value of the analytical value at which the quantification of the analyte is achieved with a certain statistical significance. In between both limits, the presence of the analyte is proven. However, a significant quantification is not possible. All decision limits are calculated from a calibration function, i.e. from the relationship between absorption and analyte concentration according to Lambert Beer`s law.
Exemplarily, Fig. 2-2 (left) depicts the Am(III) absorption spectra. Fig 2-2 (right) shows the clear linearity between the area of the absorption bands of Am(III) and the analyte concentration down to low concentrations. The detection limit (DL) and limit of determination (LoD) of Am(III), Eu(III), and Nd(III) are summarized in Tab. 2-1. The determined absorption maximum and oscillator strength are in good agreement with literature values [CAR1979, RAO1987]. Values of LD and LoD show clearly that the method is suitable for measurements in the low concentration range. However, the quality of the spectra depends on the wavelength of absorption maxima. For example, in case of Eu(III) with absorption maximum near the border of the transmission of the LPFC the baseline effects may cause a somewhat higher detection limit due to stronger noise.

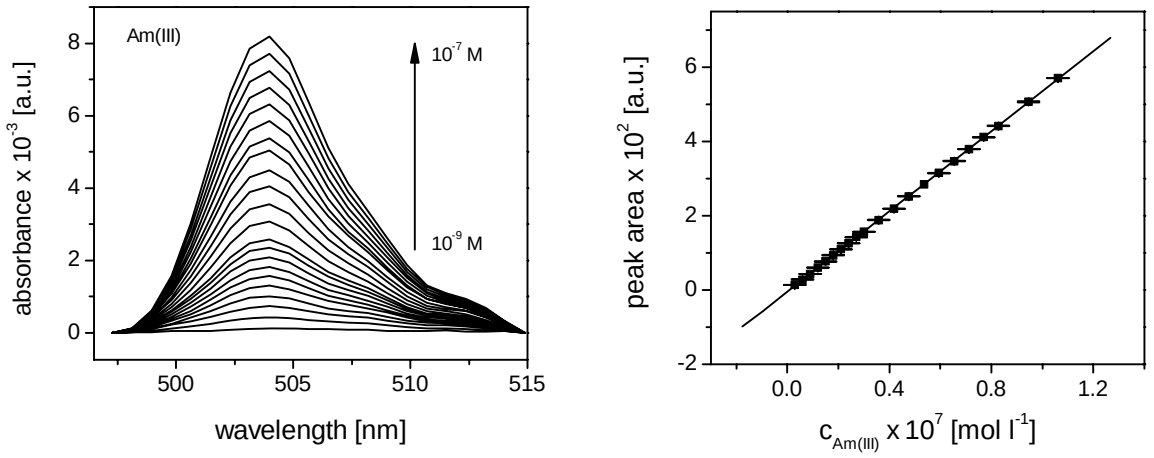

Fig. 2-2: Left: Absorption spectra of Am(III). Right: Integrated absorption signal as function of Am(III) concentration (pH = 3, 0.1 M $NaClO_4$)

Tab. 2-1: Absorption properties of Am(III), Eu(III) and Nd(III) [ACK2011]

	Am(III)	Eu(III)	Nd(III)
examined transition	$^7F_0$-$^5L_6$	$^7F_0$-$^5L_6$	$^4I_{9/2}$-$^4G_{5/2}$
determined absorption maximum [nm]	503.9	394.0	575.0
molar extinction coefficient [$M^{-1}\cdot cm^{-1}$]	393 ± 2 [MÜL2010]	2,77 [CAR1979]	7,20 [RAO1987]
determined oscillator strengths	485	1,7[a)]	9,4[a)]
detection limit (DL) [$mol\cdot L^{-1}$][b)]	$5\cdot10^{-9}$	$5\cdot10^{-6}$	$4\cdot10^{-7}$
limit of determination (LoD) [$mol\cdot L^{-1}$][b)]	$1\cdot10^{-8}$	$2\cdot10^{-5}$	$2\cdot10^{-6}$

a) values in good agreement with values published in [CAR1968, RAO2010],
b) optical path length 2 m

For temperature dependent measurements all relevant components, e.g. the LPFC and the sample were arranged in an (isolated) acrylic glass box and then brought to temperature with an Air-Therm (ATX World Precision Instruments). The Air-Therm uses hot air to heat up a fixed volume to temperatures up to 60°C. Since no cooling is possible with the Air-Therm room temperature is the lowest available temperature. The temperatures in the sample and at the LPFC were determined continuously with thermocouple elements.
The spectra of all investigated Ln(III) and Am(III) ions show a slight temperature dependence. In the studied temperature range a linear decrease in the absorption intensity and the peak area with increasing temperature is observed (Fig. 2-3 left). Unavoidable temperature differences between sample vessel and LPFC, mostly around 3K, are the major source of uncertainties. They lead to the error bars shown in Fig. 2-3 (right). The linear relationship between the analyte concentration and the peak area is not affected by temperature [SCH2008].

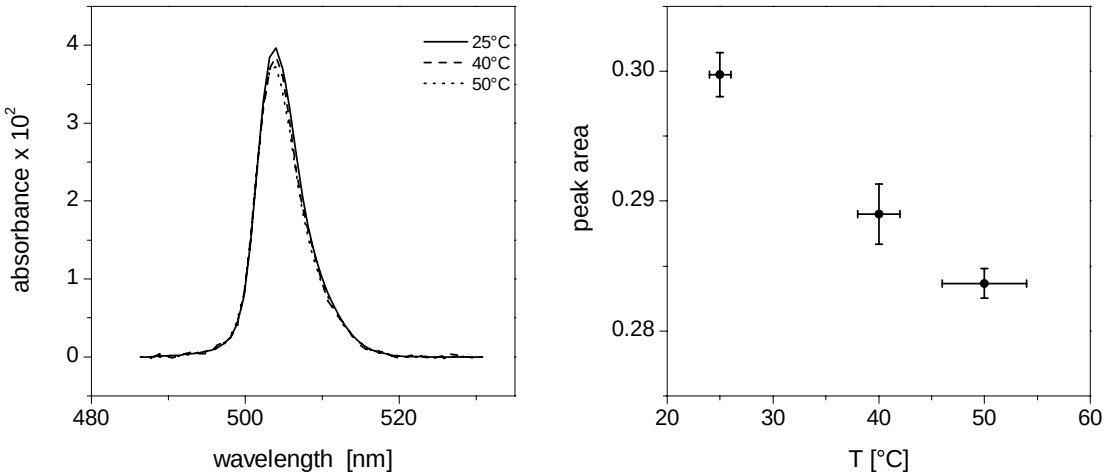

Fig. 2-3: Left: Absorption spectra of Am(III). Right: Integrated absorption signal as function of temperature (pH =3, 0.1 M $NaClO_4$, $c_{Am(III)} = 7\cdot10^{-7}$ M)

The Am(III) absorption band at 503 nm is influenced by the chemical environment due to its hypersensitivity [CAR1964]. In the majority of cases a small bathochromic shift (in nm) of the absorption band is observed caused by nephelauxetic effect [BAR1996]. Information on formed complex species can be obtained from this shift. The stability constants of Am(III)-ligand complexes were determined from spectrophotometric UV-vis titration. Solutions with $5 \cdot 10^{-7}$ M Am^{3+} in 0.1 M $NaClO_4$ (in 5 ml) and pH values between 4.0 and 5.0 were titrated with small aliquots (2 to 10 µl) of a 0.001, 0.01 or 0.1 M ligand solution (with the same pH value). 20-40 titration steps up to a ligand concentration of $1 \cdot 10^{-3}$ M were performed at the chosen temperature.

2.1.5 Data analysis and determination of complex formation constant

For both methods, UV-vis and TRLFS spectroscopy the complex stoichiometries were determined graphically using the general formula of complex formation

$$M^{3+} + n\ Lig \leftrightarrow M(Lig)_n^{3+} \tag{2-4}$$

and the corresponding mass action law

$$K = \frac{c[M(Lig)_n^{3+}]}{c[M^{3+}] \cdot c[Lig]^n} \tag{2-5}$$

followed by a slope analysis on the basis of the modified logarithmic linear form of the mass action law:

$$\log \frac{c[M(Lig)_n^{3+}]}{c[M^{3+}]} = n \cdot \log c[Lig] + \log K \tag{2-6}.$$

The concentrations of the uncomplexed and complexed species were calculated from the deconvoluted absorption or static luminescence spectra.

The complex stability constants were derived from the spectra using SPECFIT [BIN2005]. Input parameters for the data fitting were the total concentrations of the metal ion and the ligand, the pH, the known stability constants for the Eu(III) or Am(III) hydroxides [GUI2003, HUM2002b], and the pK_a values of the ligands.

Plotting temperature-dependent complex formation constants as natural logarithm versus the reciprocal temperature, the thermodynamic data parameters enthalpy (ΔH) and entropy (ΔS) were calculated from the slope and the intercept by the Van't Hoff equation in a modified linear form:

$$\ln K = -\frac{\Delta H}{R} \cdot \frac{1}{T} + \frac{\Delta S}{R} \tag{2-7}.$$

The uncertainty of all given experimental values is given as 1σ.

2.1.6 Fourier-transform infrared (FTIR) spectroscopy and Density functional theory (DFT) calculation

FTIR

FTIR spectra were recorded in aqueous phase using a Vector-22 spectrometer (BRUKER, Karlsruhe, Germany) equipped with a diamond attenuated total reflectance (ATR) unit (RESULTEC, Illerkirchberg, Germany). The ligand was measured at pH 7.0 and 100 mM pyromellitic acid. For the solution with precipitations, 20 µL 100 mM $EuCl_3$ solution (pH 7.0) was mixed with 20 µL of a 100 mM ligand solution (pH 7.0), resulting in a final concentration of $5 \cdot 10^{-2}$ M for Eu(III) and ligand each. The mixture precipitates rapidly and was therefore measured as a suspension. The monomeric complex was measured at pH 5.0, 1 mM Eu(III), 1 mM ligand and 0.1 M NaCl in a flow cell (volume: 200 µL) with a constant flow rate of 200 µL/min and the absorption difference was calculated from the spectra of the complex and the pure ligand. For every single spectra 4×256 scans were co-added. Spectral resolution was 2 cm^{-1}. Water single-channel spectra were used as reference to calculate absorption spectra.

DFT

DFT calculations were performed using Gaussian 03 [FRI2004]. Geometries were optimized in the aqueous phase at the B3LYP level using the CPCM solvation model [BAR1998] with UAHF radii [BON1964]. The large core effective core potential (LC-ECP) as well as the corresponding basis set suggested by Dolg et al. was used on Eu [DOL1989]. For C, O, and H, all-electron valence triple-zeta basis set plus polarization and diffuse functions have been used [KRI1980]. The LC-ECP used in this study is specifically designed for the trivalent Eu incorporating six unpaired 4f electrons into the core potential, thereby enabling "closed-shell" calculations on Eu(III) which has the formal electronic configuration of the septet spin state. This simplification is justified because the 4f orbital is strongly contracted, shielded by valence orbitals, and does not participate in the chemical bond between Eu(III) and the ligand. The final geometries were confirmed to be the energy minimum through vibrational frequency analysis where no imaginary frequency was found to be present. The vibrational spectra were fitted with the half-width of 8 cm^{-1} at half-height using the calculated harmonic frequencies and IR intensities.

The Spin-orbit effect and multi-configurational character of the system were neglected. Both effects are expected to be important for the accurate determination of the electronic energy levels of the Eu(III) complex. Their contributions to the ground state geometry, however, are small because 4f electrons are localized on the Eu atom in the ground state and low energy excited states and do not contribute to ligand interactions. According to the recent study on Cm(III) complexes [CAO2009], which are analogous to the Eu(III) complexes, solvation energy is the most critical factor for the determination of geometries and vibrational frequencies. The first coordination sphere around Eu was saturated with water molecules fixing the coordination number to 8 or 9. The rest of the solvation shells were also considered through the use of the CPCM model.

2.1.7 Isothermal titration calorimetry

ITC measurements were done with a Microcal VP-ITC calorimeter (GE Healthcare, Buckinghamshire, UK) at different temperatures (25, 40 and 60°C). A total of 56 aliquots (5 µl of 10 mM BTC in 0.1 M $NaClO_4$, pH 5.7) were injected in 1.412 mL of 1 mM $EuCl_3$ (0.1 M $NaClO_4$, pH 5.7) in 5 min intervals at 25°C, and in 27 min intervals at 40 and 60°C to allow the completion of slow reactions at these temperatures. The measurements were

corrected for the heat of dilution of the titrant, determined in separate runs. Measurements were analyzed with the associated software Origin 7.5.

2.2. Results and discussions

2.2.1 Potentiometric titration

In addition to the proton dissociation constants of the ligands at 25°C which are mostly literature known [POW2005] those at higher temperatures are required for the determination of Ln(III)/An(III) complex stability constants at elevated temperatures. Tab. 2-2 to 2-4 summarize the dissociation constants for pyromellitic acid, salicylic acid, and tartaric acid at elevated temperatures and the corresponding enthalpies and entropies calculated with Eq. 2-7. For ambient temperature our data are within the range of reported values. All protonation reactions are slightly endotherm (increasing pK_a values with rising temperatures). The thermodynamic data agree well with published calorimetric data at 25°C for pyromellitic acid [CHO1994, PUR1972]. Slightly negative enthalpies were published for salicylic and tartaric acid [DER1999, HAS1990a]. Possibly the different methods and temperatures (temperature dependent potentiometric titration versus calorimetry at room temperature) or the different background electrolytes (sodium perchlorate versus sodium chloride) can cause these contradictory results.

Tab. 2-2: pK_a values and thermodynamic data of pyromellitic acid (in 0.1 M $NaClO_4$) at varying temperature determined by potentiometric titration.

T [°C]	pK_{a1}	pK_{a2}	pK_{a3}	pK_{a4}	Ref.
25	1.92 ± 0.03	2.77 ± 0.03	4.36 ± 0.02	5.35 ± 0.02	this work
25		2.63	4.18	5.25	[CHO1994]
25	1.70	3.12	4.92	6.23	[PUR1972]
30	1.91 ± 0.02	2.86 ± 0.01	4.45 ± 0.01	5.43 ± 0.01	this work
40	2.05 ± 0.02	2.88 ± 0.01	4.48 ± 0.01	5.48 ± 0.01	this work
50	2.11 ± 0.01	2.88 ± 0.01	4.47 ± 0.01	5.51 ± 0.01	this work
60	2.13 ± 0.02	2.91 ± 0.02	4.50 ± 0.01	5.50 ± 0.02	this work
$\Delta_r H$ [kJ·mol^{-1}]	13.2 ± 2.2	6.0 ± 2.2	6.0 ± 2.4	7.7 ± 2.3	this work
		6.8	1.3	4.5	[CHO1994][a)]
	13.0	6.6	3.3	6.7	[PUR1972][a)]
$\Delta_r S$ [J·K^{-1}·mol^{-1}]	81 ± 7	74 ± 7	104 ± 8	129 ± 8	this work
		73	84	116	[CHO1994][a)]
	76	82	106	142	[PUR1972][a)]

a) from calorimetry (25°C)

Tab. 2-3: pK_a values and thermodynamic data of salicylic acid (in 0.1 M $NaClO_4$) at varying temperature determined by potentiometric titration.

T [°C]	pK_a	Ref
10	2.77 ± 0.01	this work
20	2.79 ± 0.01	this work
25	2.72	[HAS1989]
25	2.82	[GON1987]
30	2.80 ± 0.01	this work
40	2.83 ± 0.01	this work
50	2.85 ± 0.01	this work
60	2.87 ± 0.02	this work
$\Delta_r H$ [kJ·mol^{-1}]	4.1 ± 0.1	this work
	-4.0	[HAS1989][a)]
$\Delta_r S$ [J·K^{-1}·mol^{-1}]	67 ± 1	this work
	39	[HAS1990b][a]

a) from calorimetry (25°C)

Tab. 2-4: pK_a values and thermodynamic data of tartaric acid (in 0.1 M $NaClO_4$) at varying temperature determined by potentiometric titration.

T [°C]	pK_{a1}	pK_{a2}	
10	2.739 ± 0.003	3.906 ± 0.002	
20	2.773 ± 0.002	3.939 ± 0.001	
25	2.828	3.949	[DER1999]
25	2.850	3.968	[ARE1980]
30	2.857 ± 0.002	3.976 ± 0.001	
40	2.904 ± 0.002	3.999 ± 0.002	
50	2.883 ± 0.002	4.017 ± 0.002	
$\Delta_r H$ [kJ·mol^{-1}]	7.4 ± 1.6	5.0 ± 0.3	
	-0.5	-0.9	[DER1999][a)]
$\Delta_r S$ [J·K^{-1}·mol^{-1}]	79 ± 5		
	17	92 ± 1	[DER1999][a)]

a) from calorimetry (25°C)

2.2.2 Pyromellitic acid [BAR2011b]

The pyromellitic acid mimics the structural arrangement of carboxylates in polyphenols and serves as a model compound for the binding of heavy metals to humic acids. The formation of aggregates is typical of humic acids and prevails in pyromellitic acid and related compounds. It emphasizes their suitability as model compounds also with respect to this environmentally important but little investigated property [BAR2011b and references therein].

Europium – TRLFS

Fig. 2-4 (left) shows the spectrophotometric titration of Eu(III) with pyromellitic acid at 25°C. With increasing ligand concentration, a strong increase of the intensity of the emission of the hypersensitive $^5D_0$-$^7F_2$ transition at 615 nm is observed. The appearance of the formally forbidden $^5D_0$-$^7F_0$ transition at 579 nm indicates the deformation of the first hydration shell of

the Eu(III) ion upon complexation. Irrespective of the ligand concentration, the luminescence exhibits a mono-exponential decay despite the intrinsically different decay times for the fully hydrated and the coordinated Eu(III) ion. Due to a fast kinetic equilibration at room temperature, the observed apparent lifetime is actually a mixture of the decay rates of the excited states of both, the uncomplexed and the complexed Eu(III) species. The initial luminescence lifetime of 111 ± 4 µs (25°C), which is typical of the Eu(III)(aq) ion, increases to a constant value of 135 ± 3 µs (25°C, averaged) with more than 60 fold excess of ligand. A similar lifetime for the Eu(III)-pyromellitate system was measured by Wang et al. [WAN1999]. The measured luminescence lifetimes do not depend on temperature between 25 and 60°C (60°C: 109 ± 1 µs, Eu^{3+}(aq), and 130 ± 2 µs, averaged, Eu(III)-pyromellitate). The number of water molecules coordinating the unbound Eu(III) ion is 9.0 ± 0.5 at 25°C and 9.2 ± 0.5 at 60°C, whereas the prolonged luminescence lifetime of the complex agrees with the presence of 7.3 ± 0.5 (25°C) to 7.5 ± 0.5 (60°C) water molecules. Thus, 1 to 2 water molecules are replaced by the carboxyl oxygens upon coordination by pyromellitate.
The slope analysis according to Eq. 2-4 to 2-6 revealed a stoichiometry of the Eu(III)-pyromellitate complex close to 1:1 at all temperatures. The complex stability constants for the 1:1 complex are summarized in Tab. 2-5. The stability constant increases with temperature. The linearity of the Van't Hoff plot (Fig. 2-4, right) further shows that the enthalpy of complex formation is virtually independent of temperature (18.5 $kJ \cdot mol^{-1}$) and agrees, together with the obtained reaction entropy of 152 $J \cdot mol^{-1} \cdot K^{-1}$, with published data [CHO1994].

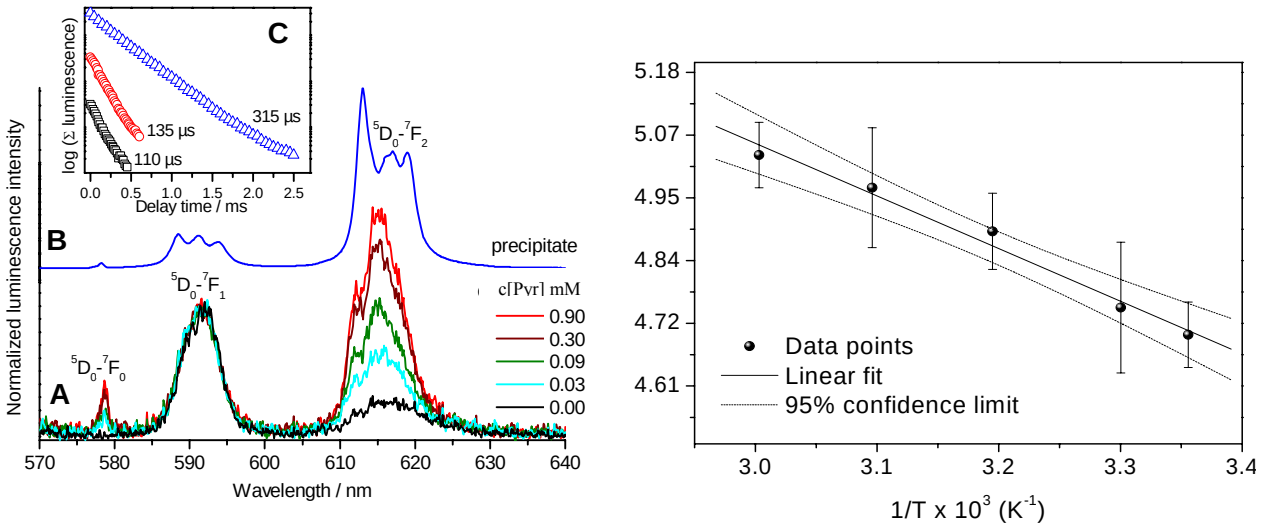

Fig. 2-4: Left : Luminescence properties of Eu(III)-pyromellitate complexes. A) Selected emission spectra of the spectrophotometric titration of 30 µM Eu(III) with pyromellitate (Pyr) (25°C, pH 5.0, 0.1 M $NaClO_4$). B) Luminescence of the precipitate forming at 1 mM Eu(III) and 1 mM pyromellitate (40 °C, pH 5.7). C) Luminescence decay traces and corresponding lifetimes of Eu(III)aq (black), Eu(III)-pyromellitate aqueous complex at 30 µm Eu(III), 4.5 mM ligand, 25°C, pH 5.0 (red), and the Eu(III)-pyromellitate precipitate (composition like B) (blue). Right: Van't Hoff plot of the Eu(III)-pyromellitate complex formation.

Eu(III) concentrations above 0.5 mM added to equimolar amounts of pyromellitate at neutral pH value caused aggregation. At 40°C and mM concentrations of both pyromellitate and Eu^{3+} aggregates formed even at pH 5.7. Figure 2-4 (left) compares the luminescence spectra of aggregates formed at equimolar concentration (1 mM) of Eu(III) and pyromellitic acid at pH 5.7, 40°C with those of the soluble complex. The $^5D_0$-$^7F_0$ peak (579 nm) is less pronounced in the aggregate, indicative of a more symmetrical structure than in solution. The lifetime of Eu(III) luminescence in the multimeric state increases to 205 ± 3 µs (pH 7.0, 25°C)

and 315 ± 5 µs (pH 5.7, 40-60°C), respectively, corresponding to 4.5 ± 0.5 and 2.8 ± 0.5 coordinating water molecules which implies the additional exchange of 2 to 4 water molecules upon aggregation of the monomeric complex.

Europium – Isothermal titration calorimetry

Isothermal calorimetric titration experiments were carried out at 25, 40 and 60°C (Fig. 2-5). All ITC traces showed endothermic binding of pyromellitate to Eu(III). The corresponding binding stoichiometries obtained from single site fits where 1.0, 1.2, and 0.9, respectively. At 25°C, the reaction enthalpy $\Delta_r H$ is (16.5 ± 0.1) kJ·mol^{-1} and the entropy $\Delta_r S$ is (130 ± 3) J·mol^{-1}·K^{-1} as derived from the ITC data in Fig. 2-5 (right). These numbers are in very good agreement with literature data [CHO1994] (Tab. 2-7). The endothermic ITC response at 25 °C was complete within less than 2 min (Fig. 2-5 left, inset). With rising temperature, however, it became biphasic with a "tailing heat uptake" resulting in an apparent $\Delta_r H$ of (34.2 ± 0.3) kJ·mol^{-1} ($\Delta_r S$ = 210 ± 9 J·mol^{-1}·K^{-1}), i.e. close to twice the molar enthalpy observed at 25°C (Fig. 2-5 right). This indicates that at higher temperatures an additional reaction succeeds the fast complex formation. Fig. 2-5 (right) exemplifies the biphasic behavior at 40°C by deconvoluting the ITC signal into a fast reaction with similar kinetics as measured at 25°C and a slower phase that covers the extra heat uptake observed at higher temperatures. The slow phase becomes further pronounced at 60°C (Fig. 2-5 right, inset). Instead of the classical evaluation of the ITC curve using a single binding reaction, it is thus reasonable to split the reaction heat separately in different time windows. It is indeed possible to divide the total heat uptake into the sum of the two isotherms shown in Fig. 2-5 (right) (lower panel). With increasing amount of Eu(III), the heat taken up in the early phase (i.e. within the first 30 seconds) is successively reduced in relation to that absorbed over the following time. This indicates that the complex reaction underlying the fast component saturates earlier than the ensuing reaction. Remarkably, the integrated heats of the early and late phase of the transient can be modeled with individual enthalpies of 14.6 and 16.3 kJ mol^{-1} (with reaction entropies of 138 and 160 J·mol^{-1}·K^{-1}, respectively, and a stoichiometry of 0.8-0.9). These values are very close to those of the 1:1 complex formation reaction at 25°C. Therefore, the data indicate that at temperatures above 40°C, the slow heat release that follows the formation of the 1:1 complex originates in an ensuing second Eu(III) coordinating interaction with thermodynamic parameters very similar to those of the fast initial complex formation. In agreement with the onset of visually observable precipitation at 40°C, the additional Eu(III) coordination appears to be crucial for the formation of polymeric states. Remarkably, the ITC data demonstrate that at 40°C an overall 1:1 stoichiometry also holds for the aggregated Eu pyromellitate complex.

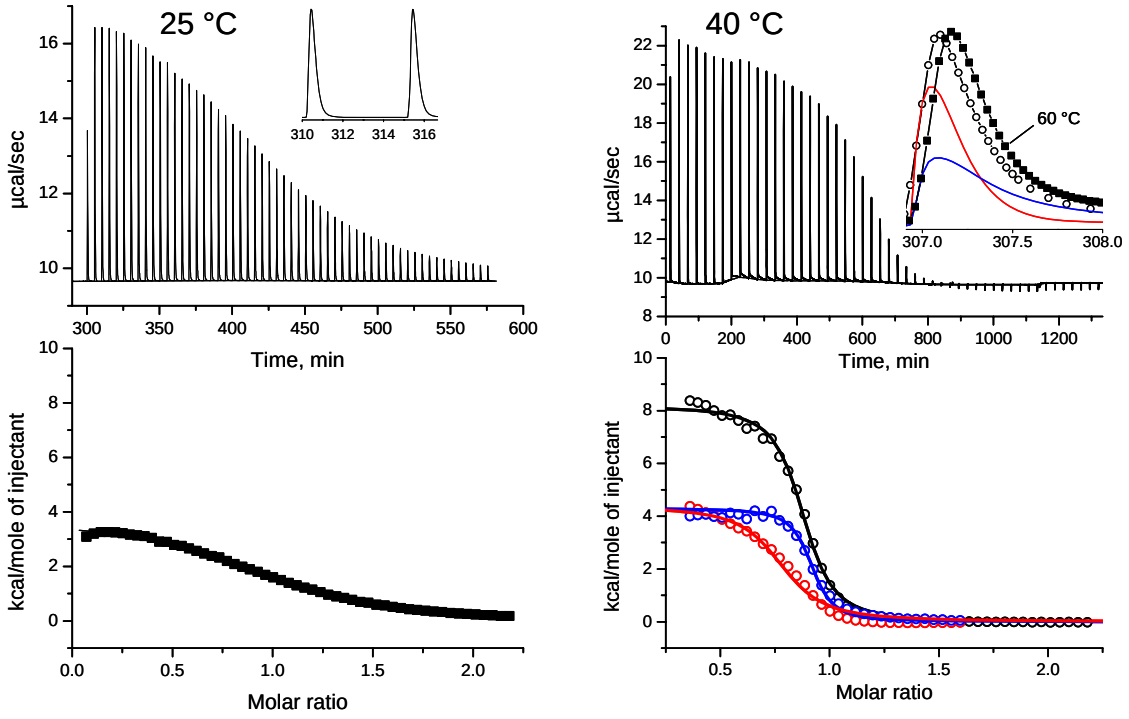

Fig. 2-5: Heat uptake during Eu(III)-pyromellitate complex formation measured by isothermal titration calorimetry at different temperatures. Explanation see text.

Europium – FTIR spectroscopy and DFT analysis

In an attempt to relate the most prominent experimentally determined vibrational features to those derived from DFT calculations for specific coordination modes, the structures of soluble (monomeric) and insoluble (polymeric) Eu(III)-pyromellitate complexes were assessed by FTIR spectroscopy at room temperature and compared with DFT calculations. It should be noted that the DFT calculations were used here to assign IR bands to the most likely predominant coordination modes and only the 1:1 complex has been calculated by DFT. The structures and IR spectra of Eu(III)-pyromellitate complexes were calculated with different coordination number (CN) of 8 and 9 and also with different coordination modes (monodentate, bidentate and chelate ring formation). The structures and relative Gibbs energies including the solvation energy are shown in Fig. 2-6. In both monodentate and bidentate complexes, the CN 8 was found to be more stable than the CN 9 by 44.6 and 33.1 kJ·mol^{-1}, respectively, which is a clear indication of CN 8 prevalence over CN 9. For the chelate ring complex, the energy difference between CN 8 and CN 9 is only 11.6 kJ·mol^{-1} and thus too small to identify a unique CN. It can also be seen in Fig. 2-6 that the energy differences among the complexes with different coordination modes and CN 8 are overall small. They all lie within the energy difference of 5 kJ·mol^{-1} and do not allow identifying a predominant coordination mode on purely theoretical grounds. It will be shown, however, that the FTIR results in combination with TRLFS data allow proposing the structural model that is most consistent with both, DFT and spectroscopy.

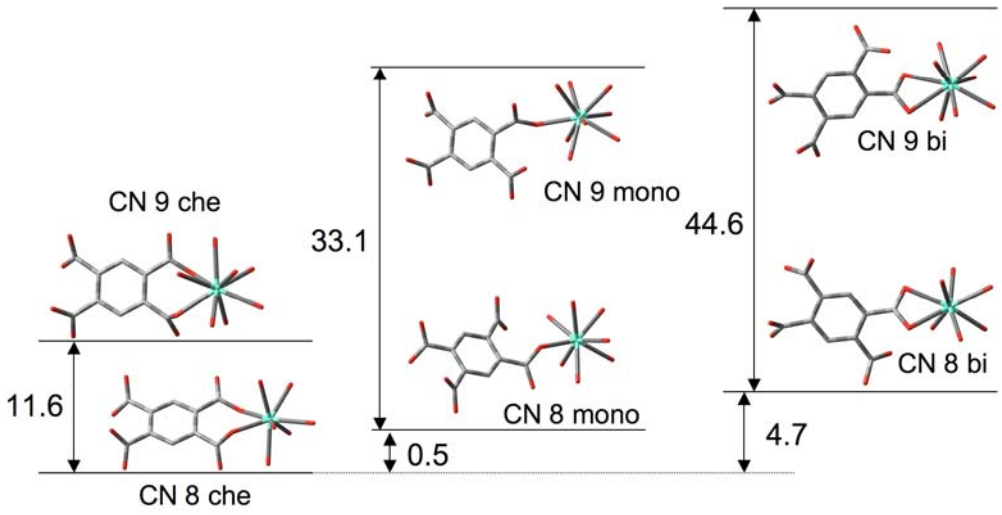

Fig. 2-6: The structures and relative Gibbs free energy [kJ·mol^{-1}] (including of the solvation) of Eu(III)-pyromellitate complex with different coordination number (CN 8 and 9) and different coordination modes (chelate, monodentate, and bidentate). Hydrogen atoms are omitted for clarity. When comparing the energy of the complexes with different number of water, one or two water molecules were added in the second coordination shell of the complex with less number of water(s).

In DFT calculations we have calculated IR spectra of the complexes with three different coordination modes (monodentate, bidentate, and chelate) and two different CN (8 and 9) (Fig. 2-7).

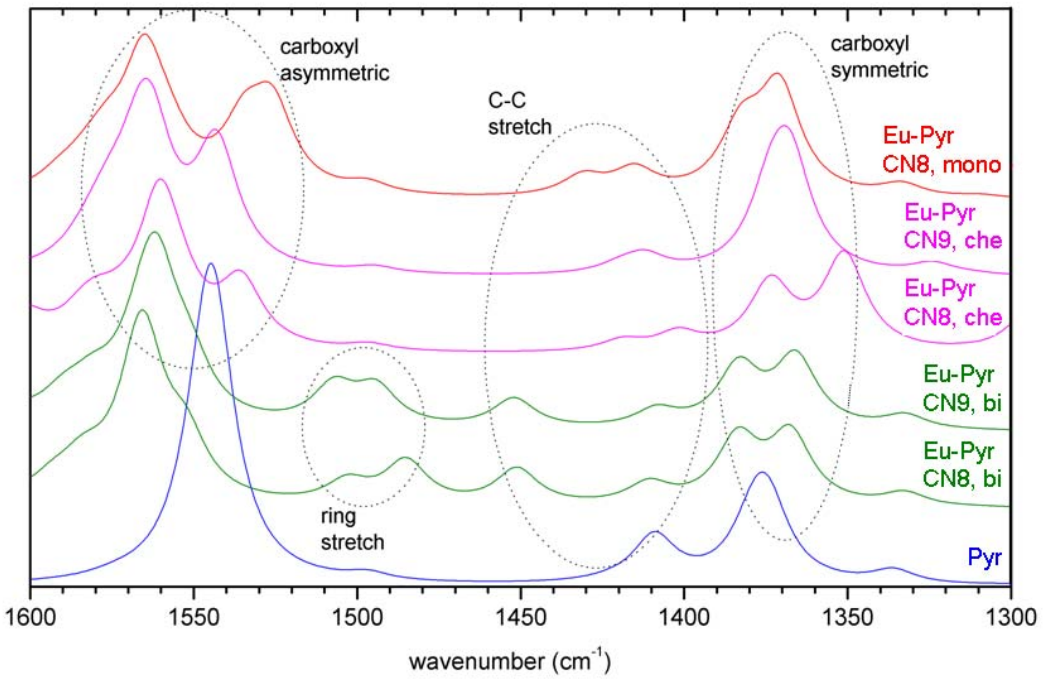

Fig. 2-7: IR spectra of pyromellitic acid and Eu(III)-pyromellitate complexes obtained by DFT calculations

Fig. 2-8 (left) shows the experimental and theoretical IR spectra of free pyromellitate (A) and pyromellitate complexed with Eu(III) ((B) monomer, (C) polymer).
Structural conclusions are based on the carboxylate vibrations as they are the most sensitive to the coordination mode. The comparison of the data of the free ligand (Fig. 2-8 A) shows that the relative positions and intensities of the calculated vibrational bands are in good accordance with the measured spectrum. DFT calculation (Fig. 2-7) shows that Eu(III) binding splits either the asymmetric (1550 to 1600 cm^{-1}) (monodentate or chelate) or the symmetric (1350 to 1400 cm^{-1}) (bidentate) carboxylate band of the ligand, leading to broad overlapping bands between 1520 and 1600 cm^{-1} and from 1350 to 1400 cm^{-1}, respectively. The bidentate coordination does not cause band splitting of the asymmetric COO^- stretch but strongly shifts it to lower frequency, whereas splitting is observed for the symmetric stretch. Such shifts and splittings will affect mainly the total band width in the 1500 to 1600 cm^{-1} range due to the broad absorption bands in the experimental spectra. The $\nu_{(as)COO-}$ stretches clearly cover a larger frequency range in the monomeric complex (Fig. 2-8 B) than in the free ligand (Fig. 2-8 A). The increased absorption above and below the $\nu_{(as)COO-}$ of the additionally present free carboxylate (Fig. 2-8, dotted line) indicates that splitting does indeed occur upon monomer formation. Thus, a bidentate coordination can be ruled out. Also the two energetically most preferred binding modes, the chelate and bidentate complexes with CN 8 each can be ruled out at least for the monomeric form due to the TRLFS results. These coordination modes would retain 6 water molecules in the first coordination shell of Eu^{3+}. This is contrary to TRLFS findings, where we found that 7 to 8 water molecules remain after complexation. Instead, the two DFT spectra which agree best with experiment are shown in Fig. 2-8. These are the chelate complex with CN 9 corresponding best with the monomer absorption (Fig. 2-8 B) and the monodentate complex with CN 8 corresponding best with the polymer (Fig. 2-8 C). In the latter, the splitting is even broader (as is the total band width in the experimental spectra) leading to a more distinct low frequency $\nu_{(as)COO-}$ stretch at 1530 cm^{-1} also seen experimentally. Additionally, a high frequency shoulder is produced in the $\nu_{(s)COO-}$ band both in the calculated and measured spectra. These most likely predominant coordination modes support our TRLFS data, which show that a chelating coordination requires a CN 9 and that 7 to 8 water molecules still remain in the first coordination shell of Eu^{3+} in the monomeric complex. The large experimental bandwidth indicates that multiple coordination modes exist in both the monomer and polymer (see Fig. 2-8, right).

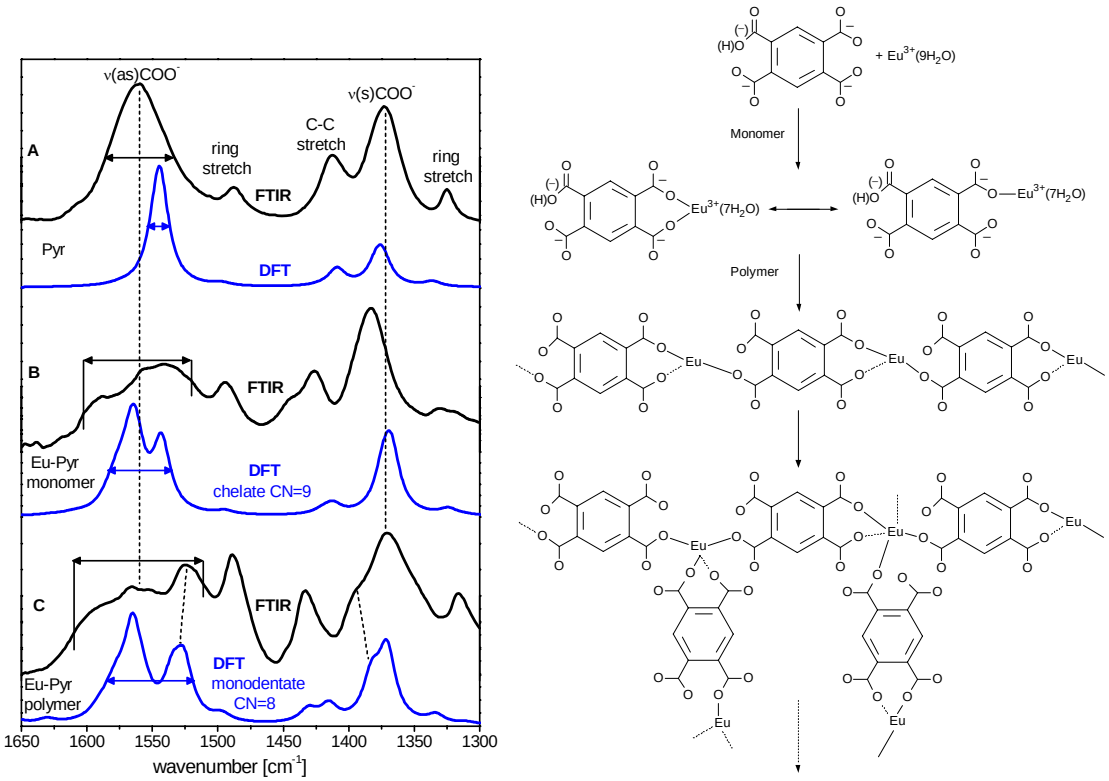

Fig. 2-8: Left: Comparison of experimental (black) and theoretical IR spectra (blue, derived from DFT calculations of pyromellitate (Pyr) and Eu(III)-pyromellitate (Eu-Pyr) complexes). **A)** Pyromellitate in 0.1 M $NaClO_4$ without europium. **B)** Eu(III)-pyromellitate complex under conditions of a prevalent monomeric state of 1:1 stoichiometry. **C)** Eu(III)-pyromellitate complex under polymerizing conditions with 1:1 stoichiometry.
Right: Schematic description of the stepwise formation of the Eu(III)-pyromellitate polymer demonstrating possible chelating and monodentate binding modes and the prevalence of a 1:1 stoichiometry in both the monomeric and polymeric states. For clarity, values, protons and water molecules are omitted in the polymeric structures.

Americium - TRLFS

Fig. 2-9 depicts a summary of the measured fluorescence spectra of the Am(III)-pyromellitate system at fixed Am^{3+} concentration (2 µM), fixed pH (5.0), and varying ligand concentration (1 µM to 90 µM). For Am^{3+}(aq) we observe the emission of the $^5D_1$-$^7F_1$ transition at 691 nm. With increasing ligand concentration no shift of the peak maximum but an increase of the luminescence intensity is observed, indicating a complex formation. The intensity remains nearly equal at more than approximately 30-fold ligand excess, where the complexation seems to be completed. The intensity development at 691 nm is depicted in Fig.2-9 as an insert.

At any studied Am(III)-ligand mixture, we observe mono-exponential decay. The initial lifetime of Am^{3+}(aq) of 23.2 ± 2.2 ns is in very good accordance with literature data (23 ± 2 ns [RUN2000], 24.6 ± 0.6 ns [KIM1998], 25.0 ± 0.8 ns [KIM2001]). The number of the associated hydration water molecules in the inner coordination sphere, calculated with Eq. 2-3, is 9.6 ± 0.5. With increasing ligand concentration the lifetime increases due to complex formation until an approximately constant value of 27.2 ± 1.2 ns at 30-fold ligand excess. The lifetime of the Am(III)-pyromellitate complex species corresponds to 8.0 ± 0.5 water molecules remaining in the inner coordination sphere of Am (considering the error of the lifetime), indicating the replacement of 1-2 water molecules through ligand coordination sites. A stoichiometry of the Am(III)-pyromellitate complex species of 1:1 was derived from the slope analysis by Eq.2-4 to 2-6 (slope of 1.26 ± 0.11). The stability constant of this complex, which is un-known until now, was calculated to be log β_{110} = 5.42 ± 0.16 (Tab. 2-6).

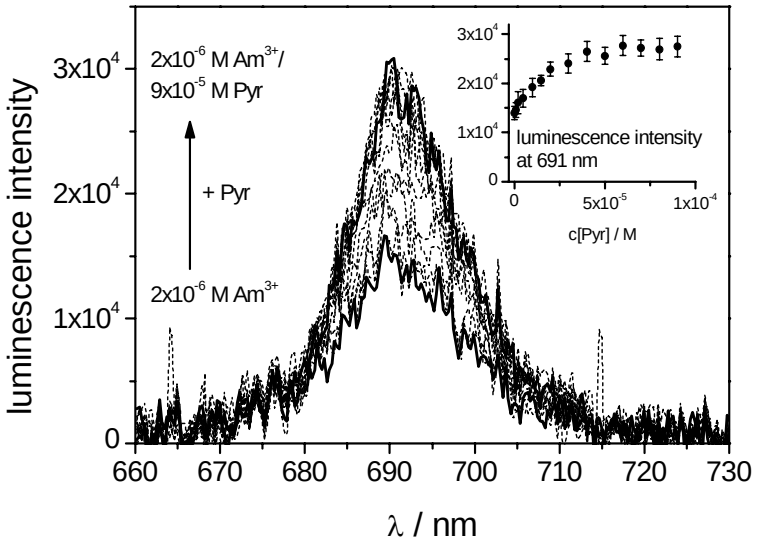

Fig. 2-9: TRLFS spectra of 2 µM Am(III) in dependence of pyromellitate concentration (pH = 5.0, I = 0.1 M $NaClO_4$, T = 21 ± 1°C). Small insert: Luminescence intensity at 691 ± 1 nm in dependence of the ligand concentration.

Americium –UV-vis

Fig. 2-10 shows the absorption spectra of Am(III) with stepwise addition of the pyromellitic acid. The ligand concentration was varied between 10^{-6} and 10^{-3} M. The spectra exhibit a slight bathochromic shift induced by ligand addition. Additionally the maximum absorption intensity changes in two different ways. It decreases first and rises again after further addition of the ligand. The shifting of absorption band clearly indicates a complex formation with the carboxylate ligand. The formation of two complex species (1:1 and 1:2 complexes) was indicated by slope analysis (Eq. 2-4 to 2-6). The 1:1 complex exhibits a slightly decreased absorption. The 1:2 complex species has an absorption maximum at 504.8 nm and slightly higher extinction coefficient.

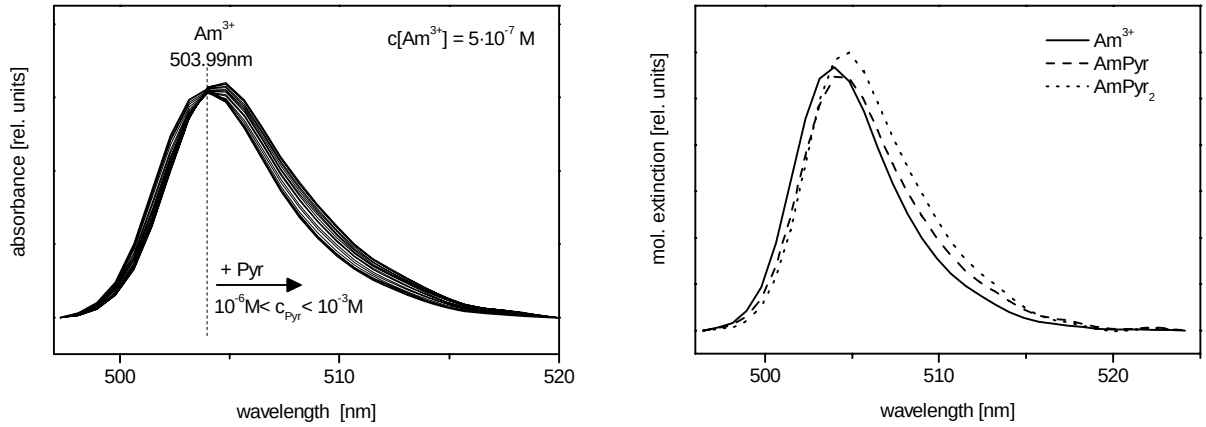

Fig. 2-10: Left: UV-vis absorption spectra of Am(III) at 25°C, pH = 5.0 and I = 0.1 M $NaClO_4$ in dependence of pyromellitate concentration (varied from 10^{-6} to 10^{-3}). Right: single component spectra determined with SPECFIT.

The spectrophotometric titration experiments were repeated at increased temperatures up to 55°C and no significant deviations from the presented trend were observed. The Van't Hoff plots, shown in Fig. 2-11, reveal always a linear relationship. The derived thermodynamic data are listed in Tab.2-6.

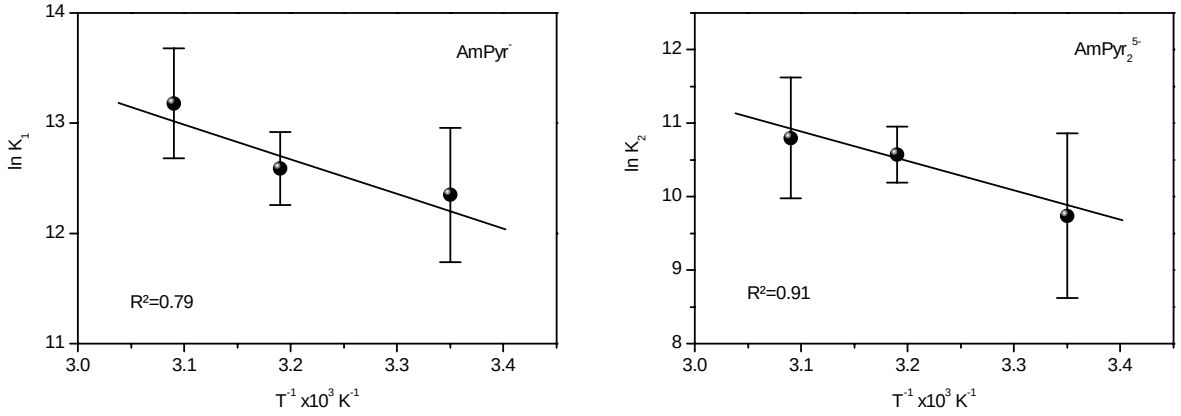

Fig. 2-11: Van't Hoff plots of the Am(III)-pyromellitate complex formation determined by UV-vis spectroscopy. Left: 1:1 complex. Right: 1:2 complex

Thermodynamic data of Eu(III) and Am(III) complexation with pyromellitic acid

In Tab. 2-5 to 2-7 the complex stability constants and derived thermodynamic data of the system Eu(III)/Am(III)-pyromellitic acid are summarized. It can be concluded that the formation of Am(III)-and Eu(III)-pyromellitate complexes are endothermic and driven by entropy. For the first time the complex stability constants of the 1:1 and 1:2 Am(III)-pyromellitate complexes were derived from spectroscopic measurements. Until now no literature data are available. However, the obtained values are in the same order of magnitude as those reported for the analogue Eu(III) (see Tab. 2-5 and 2-7) [BAR2011b] or Nd(III) complexes [ZES2011].

Tab. 2-5: Complex stability constants at varying temperature for the monomeric 1:1 Eu(III)-pyromellitate complex (I = 0.1 M $NaClO_4$) determined by TRLFS.

T [°C]	$\log\beta_{110}$	Ref.
25	4.70 ± 0.06	this work
25	4.86 ± 0.03	[CHO1994][a)]
30	4.75 ± 0.12	this work
40	4.89 ± 0.07	this work
50	4.97 ± 0.11	this work
60	5.03 ± 0.06	this work

a) from potentiometric titration

Tab. 2-6: Thermodynamic data for Am(III)-pyromellitate complexes (I = 0.1 M $NaClO_4$) determined by UV-vis and TRLFS

T [°C]	$\log\beta_{110}$	$\log\beta_{120}$	method	Ref.
20	5.42 ± 0.16	-	TRLFS	this work [BAR2011a]
25	5.4 ± 0.3	9.74 ± 1.12	UV-vis	this work
40	5.5 ± 0.1	10.57 ± 0.38	UV-vis	this work
50	5.7 ± 0.2	10.80 ± 0.82	UV-vis	this work
$\Delta_r H$ [kJ·mol^{-1}]	26 ± 13	33 ± 10	UV-vis	this work
$\Delta_r S$ [J·K^{-1}·mol^{-1}]	189 ± 43	139 ± 33	UV-vis	this work

Tab. 2-7: Summary of the thermodynamic data for the 1:1 Eu(III)-pyromellitate complex (I = 0.1 M $NaClO_4$).

T [°C]	Δ_rH [kJ·mol^{-1}]	Δ_rS [J·K^{-1}·mol^{-1}]	Δ_rG [kJ·mol^{-1}]	method	Ref.
25-60	18.5 ± 1.5	152 ± 5	-26.8 (25 °C)[a)]	TRLFS	this work [BAR2011b]
25	17.0 ± 1.6	150 ± 1	-27.7	ITC	[CHO1994]
25	16.5 ± 0.1[b)]	130 ± 3	-22.2	ITC	this work
40	34.2 ± 0.3[b),c)]	210 ± 9	-31.5	ITC	this work
60	46.9 ± 0.2[b),c)]	247 ± 9	-35.4	ITC	this work

a) calculated with the formula $\Delta_rG = \Delta_rH - T\,\Delta_rS$.
b) $\Delta Cp = 0.9$ kJ·mol^{-1}·K^{-1} was calculated from $\Delta H/\Delta T$.
c) apparent values (explanation in chapter Eu-Isothermal titration calorimetry)

2.2.3 Salicylic acid

Europium - TRLFS

The complexation of Eu(III) with salicylate was studied with TRLFS in the temperature range between 25°C and 60°C. The luminescence spectrum of Eu(III) shows in presence of the ligand the typical changes which indicate a complexation: The intensity of the hypersensitive $^5D_0$-$^7F_2$ transition at about 615 nm increases strongly, the symmetry-forbidden $^5D_0$-$^7F_0$ transition appears (see Fig. 2-12, right), and the luminescence lifetime prolongs. The luminescence lifetimes of the Eu(III)aquo ion are nearly similar within the studied temperature range (115 ± 2 µs at 25°C or 109 ± 2 µs at 55 °C). Applying Eq. 2-2, the lifetimes correspond to a number of 9 water molecules in the first spherical coordination shell of Eu(III) (8.6 ± 0.5 at 25°C and 9.2 ± 0.5 at 55°C). The luminescence lifetime is prolonged with ligand addition and reaches a constant value with more than 0.05 M salicylate of about 305 ± 5 µs. This corresponds to a number of 3 remaining water molecules in the first coordination shell of Eu(III); 6 water molecules has been substituted by coordination sites of ligand molecules. A similar lifetime (about 300-340 µs) was found by Kuke et al. [KUK2010] for a concentrated Eu(III) salicylate mixture at decreased temperatures (80-200 K); at room temperature they observed quenching contributions, possibly due to the high concentration of both metal and ligand.

Salicylate can act as unidentate or chelating ligand, either with bidentate coordination of the carboxylate group or with a monodentate coordination of the carboxylate and an additional coordination of the hydroxyl group [KUK2010, TOR2005]. A theoretical study on the molecular structure of Eu-salicylate complexes in aqueous system revealed that the 1:1 carboxylate-coordinated complex takes unidentate coordination with 8 remaining water molecules in the first coordination shell of Eu(III), but also an intra-molecular chelate ring closure with the OH group under replacement of 3 water molecules seems to be possible. A bidentate coordination of the carboxylate group was excluded due to the higher formation energy [TOR2005]. The substitution of up to 6 water molecules in the first coordination shell of Eu(III) upon complexation with salicylate suggests the formation of more than a 1:1 complex. Also complexes with 1:2 and 1:3 metal-to-ligand stoichiometry seem to be formed. The high water substitution rate implies furthermore the formation of chelate coordination with carboxylate and (protonated) hydroxyl; a unidentate coordination mode seems to be unlikely. These assumptions are underlined by a crystal structure of $Eu(Sal)_3$ where both the carboxylate and hydroxyl group coordinate the metal ion in a chelating manner [KUK2010].

The stoichiometry of the formed complexes was calculated with slope analysis according to Eq. 2-4 to 2-6. At 25°C, up to approximately 0.01 M salicylate a slope of 0.7 ± 0.1 suggests the dominance of the 1:1 complex $EuSal^{2+}$, whereas with higher ligand concentration the

slope of 1.8 ± 0.2 indicates the formation of the 1:2 complex $Eu(Sal)_2^+$. The average slope over the whole measured concentration range is 1.3 ± 0.2. With higher temperatures the slope at higher ligand concentration increases slightly up to 2.0 ± 0.2 (55°C) and the average slope increases up to 1.7 ± 0.1 (60°C). Provided that the formation of the 1:1 and 1:2 complexes occur in this region a formation of a 1:3 complex $Eu(Sal)_3$ seems to be reasonable.
The complex stability constants for these 3 complexes could be determined in the studied temperature range between 25°C and 60°C (Tab. 2-8). Up to date only the stability constants for the 1:1 and 1:2 complexes and only at room temperature have been determined [AOY2004, HAS1989, IRV1970]; the 1:2 complex was observed only once [HAS1989]. The literature values are somewhat higher than ours (see Tab. 2-8). This is possibly due to a small amount of undetected 1:3 complex, which might be enlarged apparently the constants of the 1:1 and 1:2 complexes. The thermodynamic data of the complexes calculated from the Van't Hoff plot depicted in Fig. 2-12 (right) are listed in Tab. 2-8.
The values indicate that the formation of the 1:1 complex is nearly temperature independent. In accordance with the literature the reaction enthalpy $\Delta_r H$ is close to zero within the error bars [HAS1990]. The formation of the 1:2 complex is slightly endothermic (similar to the literature value [HAS1990]), and the 1:3 complex is even stronger endothermic. This might be an explanation why this complex was not detected at room temperature so far.

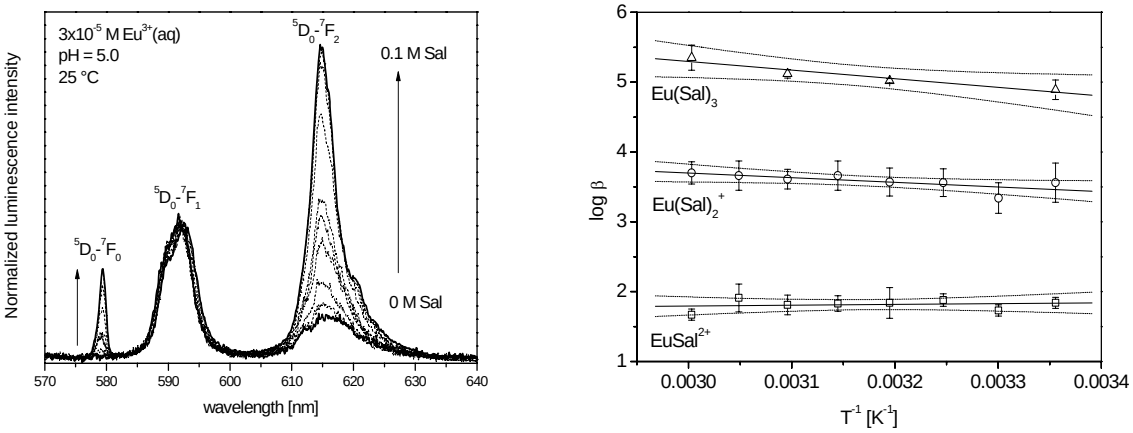

Fig. 2-12: Left: Luminescence emission spectra of the spectrophotometric titration of $3 \cdot 10^{-5}$ M Eu(III) with 0.001-0.1M salicylate (25°C, pH = 5.0, I = 0.1 M $NaClO_4$). Right: Van't-Hoff plot of the Eu(III)-salicylate complex formation.

Thermodynamic data of complexation of Eu(III) and Am(III) with salicylic acid

For the first time a 1:3 Eu(III)-salicylate complex was identified and thermodynamically characterized. With increasing complex stoichiometry the complexation enthalpies and entropies increase (Tab. 2-8). This indicates, that the formation of the 1:2 and particulary the formation of the 1:3 complexes are more driven by entropy than the 1:1 complexes.
Furthermore, Tab. 2-8 contains the data of the complexation of Am(III) with salicylic acid, published by Müller et al [Mül2010]. These complexes were UV-vis-spectroscopically identified and thermodynamically characterized for the first time.

Tab. 2-8: Stability constants at varying temperatures and thermodynamic data of Eu(III)/Am(III) complexes with salicylate determined by TRLFS (I = 0.1 M $NaClO_4$).

Am(III)				
T [°C]	$\log\beta_{110}$	$\log\beta_{120}$	$\log\beta_{130}$	Ref.
25	2.56 ± 0.08	3.93 ± 0.19		this work [MÜL2010][a)]
Eu(III)				
T [°C]	$\log\beta_{110}$	$\log\beta_{120}$	$\log\beta_{130}$	Ref.
25	2.02	3.84		[HAS1989]
25	2.08			[AOY2004]
25	2.59			[IRV1970]
25	1.84 ± 0.08	3.56± 0.28	4.89 ± 0.14	this work
30	1.73 ± 0.08	3.34 ± 0.22		this work
35	1.88 ± 0.09	3.56 ± 0.20		this work
40	1.84 ± 0.22	3.57 ± 0.15	5.02 ± 0.13	this work
45	1.83 ± 0.11	3.66 ± 0.21		this work
50	1.81 ± 0.14	3.61 ± 0.22	5.12 ± 0.16	this work
55	1.91 ± 0.14	3.66 ± 0.21		this work
60	1.67 ± 0.08	3.70 ± 0.16	5.35 ± 0.18	this work
$\Delta_r H$ [kJ·mol^{-1}]	-2.14 ± 4.9 1.3[b)]	12.7 ± 4.8 5.7[b)]	23.7 ± 4.9	this work [HAS1990]
$\Delta_r S$ [J·K^{-1}·mol^{-1}]	28 ± 15	109 ± 15	172 ± 16	this work

[a)]UV-vis with LPFC [b)] from calorimetry (25°C)

2.2.4 Lactic acid

Lactic acid is an alpha hydroxyl acid, which is considered as ubiquitous in environment. It can be regarded as decomposition product of larger molecules, e.g. humic acids and is an important intermediate in metabolism. Furthermore it is used in large amount in food industry. Due to its prominence it is used as model ligand for complex formation with various metal ions [TIA2010].

Europium - TRLFS

Fig. 2-13 (left) shows the luminescence spectra of Eu(III) with lactate. With increasing ligand concentration we observe the spectral changes which are typical for complex formation: strong increase of the intensity of the hypersensitive $^5D_0$-$^7F_2$ transition at about 615 nm, appearance of the symmetry-forbidden $^5D_0$-$^7F_0$ transition, and a prolongation of the luminescence lifetime. This general behavior remains equal within the temperature range between 25 and 70°C and between pH 5 and 6. The luminescence lifetime increases from 111 ± 2 µs for the Eu(III) aquo ion up to 225 ± 2 µs at 0.1 M lactate. This corresponds to a number of 5 remaining water molecules; 4 water molecules have been removed upon complexation with lactate. This is in good accordance to literature, where a luminescence lifetime of 197 µs for the highest lactate concentration was observed [TIA2010]. Following the interpretation of Tian et al. [TIA2010], that the hydroxyl group of lactate is involved in

the coordination of the Eu^{3+} ion and about 1.5 water molecules are exchanged through 1 lactate it is assumed that 1:1, 1:2 and 1:3 Eu(III)-lactate complexes are formed. The stability constants of these 3 complexes were determined for various temperatures (Tab. 2-9) and with Eq. 2-7 thermodynamic data were determined (Tab. 2-9 and Fig. 2-13). Whereas the formation of the 1:1 and 1:2 complexes are nearly temperature independent, the 1:3 complex formation reaction is slightly exothermic. In contrast, Tian et al. [TIA2010] observed exothermic formation reactions for all 3 complexes. Indeed, they carried out their experiments at an ionic strength of 1.0 M. This difference is possibly caused by the different ionic strengths. A possible relationship between thermodynamic data and the ionic strength will be a topic in the following project.

Americium – TRLFS

The Am(III) aquo ion shows at pH 3-6 and between 25 and 65°C a luminescence lifetime of 23.2-23.8 ns. Applying Eq. 2-3, this corresponds to approximately 9 coordinating water molecules. Complexation with lactate causes a strong increase of the luminescence intensity and a red shift of the luminescence maximum of about 5 nm (Fig. 2-13, right). The luminescence lifetime is prolonged up to 37 ns which corresponds to 5-6 remaining water molecules, indicating an exchange of about 3-4 water molecules with coordination sites of ligand molecules, similar to the Eu-lactate system, which implies the formation of 1:1, 1:2 and 1:3 complexes.

The slope analysis applying Eq. 2-4 – 2-6 shows that up to a lactate concentration of 0.01 M mainly the 1:1 complex is formed. At higher ligand concentration additionally the 1:2 and 1:3 complexes are coexistent. We were not able to separate these higher complexes. Therefore we only determined the stability constant of the 1:1 complex at various temperatures and derived the thermodynamic data of this complex (Tab. 2-9 and Fig. 2-14). The values are in very good agreement with those of the Eu(III)-lacte 1:1 complex.

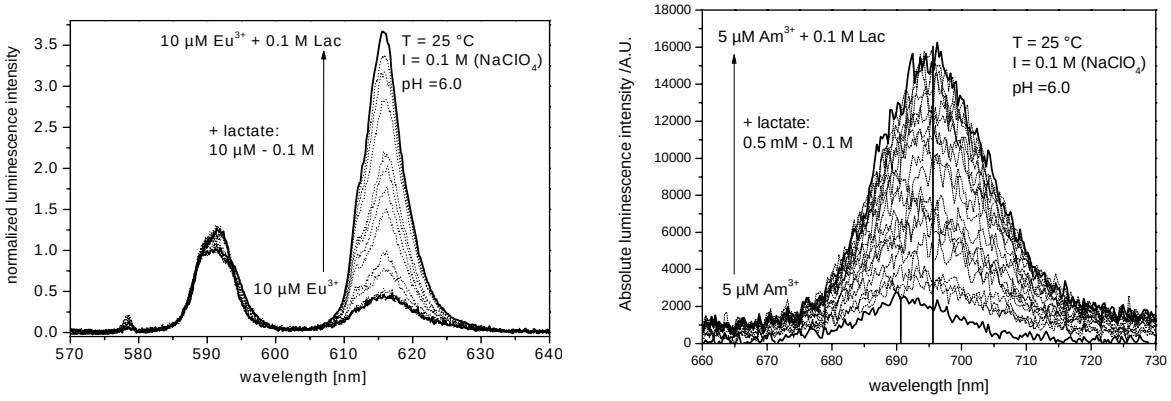

Fig. 2-13: Left: Luminescence emission spectra of the spectrophotometric titration of $1 \cdot 10^{-5}$ M Eu(III) with lactate (25°C, pH = 6.0, I = 0.1 M $NaClO_4$). Right: Luminescence emission spectra of the spectrophotometric titration of $5 \cdot 10^{-6}$ M Am(III) with lactate (25°C, pH = 6.0, I = 0.1 M $NaClO_4$).

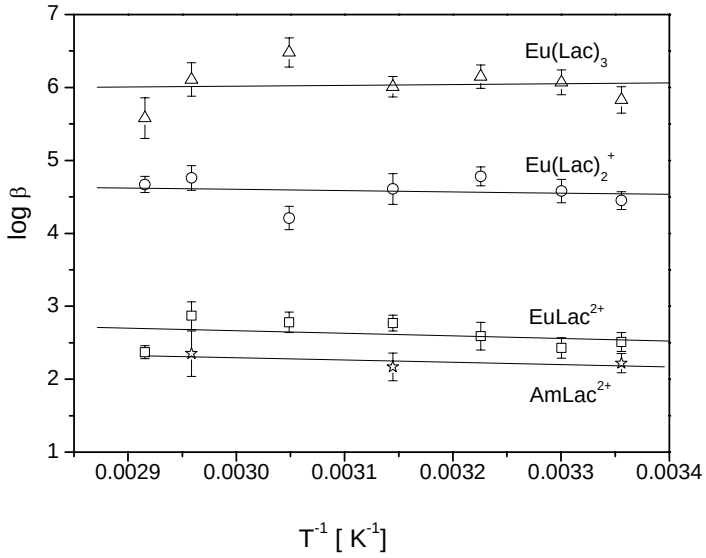

Fig. 2-14: Van't-Hoff plots of the Eu(III) and Am(III) lactate complex formation determined by TRLFS

Americium – UV-vis

Fig. 2-15 (left) shows the absorption spectra of Am(III) with increasing ligand concentration. The addition of ligand induces a slight bathochromic shift of the absorption band. Until a ligand concentration of 10^{-3} M the shift is smaller than 1 nm. This shift is a clear hint for complex formation (Fig. 2-15 right).

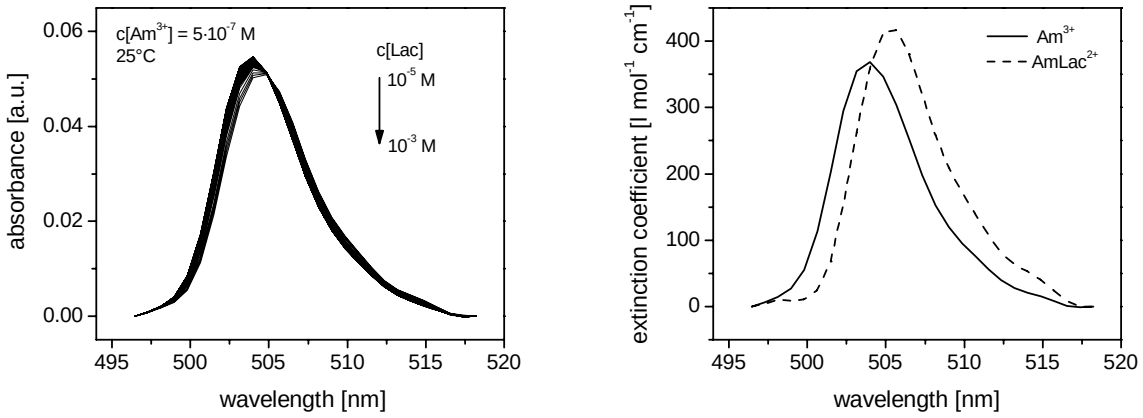

Fig. 2-15: Left: UV-vis absorption spectra of Am(III) at pH 5.0 and 0.1 M $NaClO_4$ with increasing ligand concentration at 25°C. The slight decrease of the Am(III) absorption is caused by dilution effects during spectrophotometric titrations. Right: single component spectra determined with SPECFIT.

The model free factor analysis provided by SPECFIT as well as the slope analysis indicate the formation of one complex species within the investigated concentration range. The complex stability constants determined from the measurements at 25°C and 50°C are listed in Tab. 2-9 and indicate an endothermic reaction. This is in agreement with the results from TRLFS as well as with the findings for the analogue Eu(III) complex.

Thermodynamic data of complexation of Eu(III) and Am(III) with lactic acid

Tab. 2-9: Stability constants at varying temperatures and thermodynamic data of Eu(III) and Am(III) complexes with lactate determined by TRLFS and UV-vis (I = 0.1 M $NaClO_4$).

system	$Am(Lac)^{2+}$	$Eu(Lac)^{2+}$	$Eu(Lac)_2^{+}$	$Eu(Lac)_3^{+}$	Ref.
T [°C]	$log\beta_{110}$	$log\beta_{110}$	$log\beta_{120}$	$log\beta_{130}$	
25	2.22 ± 0.13	2.51 ± 0.13	4.45 ± 0.12	5.83 ± 0.18	this work
	2.24 ± 0.04 [a]				this work [a]
		2.80	4.76	6.33	[TIA2010][c]
	2.43				[LUN1984][b],[c]
30		2.43 ± 0.14	4.58 ± 0.16	6.07 ± 0.17	this work
37		2.59 ± 0.19	4.78 ± 0.13	6.15 ± 0.16	this work
45	2.17 ± 0.19	2.77 ± 0.11	4.61 ± 0.21	6.01 ± 0.14	this work
50	2.75 ± 0.04 [a]				this work [a]
55		2.78 ± 0.14	4.21 ± 0.16	6.48 ± 0.20	this work
65	2.35 ± 0.31	2.87 ± 0.19	4.76 ± 0.17	6.11 ± 0.23	this work
70		2.37 ± 0.09	4.67 ± 0.11		this work
Δ_rH [kJ·mol^{-1}]	6.0 ± 6.6	6.7 ± 9.2	3.3 ± 1.3	-2.1± 1.6	this work
	-16				[LUN1984][c],[d]
		-2.1	-4.3	-12.4	[TIA2010][c],[d]
Δ_rS [J·K^{-1}·mol^{-1}]	62 ± 20	28 ± 15	109 ± 15	172 ± 16	this work
	-6				[LUN1984][c],[d]
		46	76	78	[TIA2010][c],[d]

[a] UV-vis with LPFC, not used for Vant' Hoff plot [b] solvent extraction. [c] I = 1 M ($NaClO_4$). [d] calorimetry

2.2.5 Citric, tartaric, and acetic acid

The further organic compounds acetic, tartaric, and citric acids also occur in the environment and therefore are widely used as model ligands for natural organic matter. Tartaric and citric acid are hydroxyl carboxylic acids with two and three carboxyl groups, respectively. The hydroxyl groups are non-dissociated until pH > 12 and do not contribute to the complex formation in the considered pH range between 4 and 5. Under the studied conditions at pH = 5 the deprotonation of three carboxylic groups of citric acid yields to the relevant species $CitH_2^-$ with two protons, $CitH^{2-}$ with one proton, and the deprotonated form Cit^{3-}. Several authors suggest that the fully deprotonated species Cit^{3-} are the predominant ligands in the formed Ln(III)/Am(III) complexes [MAT2007, OHY1971, EBE1972, HUB1974, HEL2010]. In contradiction, under the given conditions the single protonated species $CitH^{2-}$ has the highest concentration compared to the other species.
For the acetic and tartaric acid only the entirely deprotonated species are relevant in the investigated pH range.

The complexation of Am(III) with these three acids were studied by UV-vis absorption spectroscopy with LPFC only. As already found for pyromellitic acid, salicylic acid [MÜL2010], and lactic acid a small red shift of the Am(III) and Eu(III) absorption bands were found with increasing concentrations of acetic, tartaric, and citric acid.

Fig. 2-16 shows exemplarily the Am(III) absorption spectra with increasing citric acid concentration at pH 5 and an ionic strength of 0.1 M $NaClO_4$. Two different species were

identified within the spectra. The absorption spectrum of the first species is shifted about 1 nm and the second species about 2 nm in comparison to the Am(III) aquo ion. The species are designated as 1:1 and 1:2 complex species and are assumed to be formed by the fully deprotonated Cit^{3-} species. The spectrophotometric titration was performed at different temperatures between 25 and 50°C and the corresponding stability constants were calculated using SPECFIT.

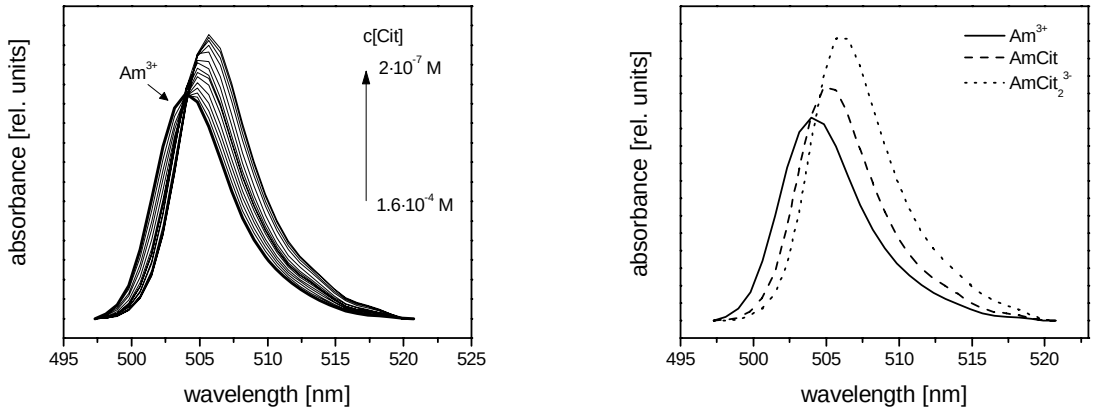

Fig. 2-16: Left: UV-vis absorption spectra of Am(III) at 25°C, pH 5.0 and I = 0.1 M $NaClO_4$. The Am(III) concentration is fixed at $5 \cdot 10^{-7}$ M. Right: single component spectra determined with SPECFIT.

The thermodynamic parameters listed in Tab. 2-10 were calculated from the Van't Hoff plots in Fig. 2-17. The values show considerable uncertainties and the linear relationship between the two quantities is of poor quality, as indicated by the quite low R^2. Heller, who studied the complexation with Eu(III) under similar conditions assumed that several Eu(III) citrate complexes with different numbers of ligands and, furthermore, with ligands of different degree of protonation are formed at this pH [HEL2010]. However, it is yet unclear if the shift originated by different protonated Am(III) complex species is pronounced enough so that different complexes can be identified or even distinguished from each other. An evidence for the existence of an AmCitH species at pH 5 was obtain by spectrometric pH titration at constant Am(III) and ligand concentration (Fig 2-18).

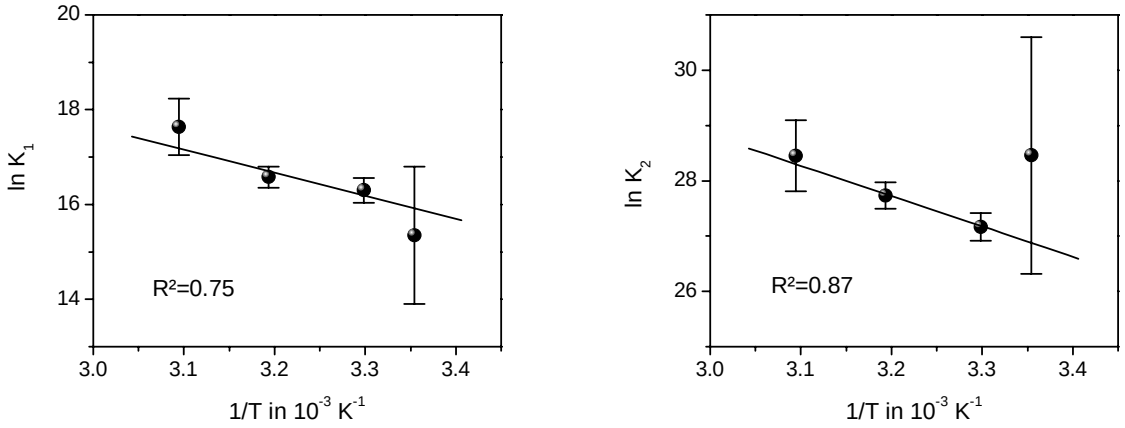

Fig. 2-17: Van't Hoff plots of the Am(III)-citrate complex formation determined by UV-vis spectroscopy. Left: 1:1 complex. Right: 1:2 complex

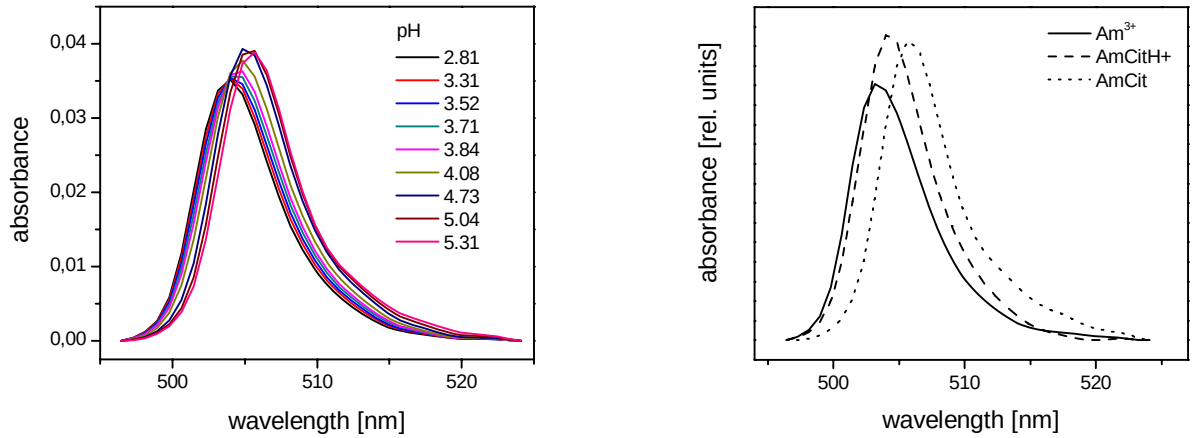

Fig. 2-18: Left: UV-vis absorption spectra of Am(III) at 25°C as function of pH and I = 0.1 M $NaClO_4$. The Am(III) concentration is fixed at $5 \cdot 10^{-7}$ M. Right: single component spectra determined with SPECFIT.

Fig. 2-18 shows pH dependent spectra of $5 \cdot 10^{-7}$ M Am(III) solution with 10^{-5} M citric acid at 25°C. At pH below 3 no complexation is observed. At pH 3.5 a clear red shift of the absorption band to higher wavelength and higher absorption occurs. At pH 4 a sudden, strong bathochromic shift and a significant decrease in absorption is found. This is a clear hint for the existence of a second complex species. It is unresolved yet, if this can either be attributed to a changed complex stoichiometry, i.e. a 1:2 complex, or to a 1:1 complex with a probably deprotonated ligand. Further measurements at lower ligand concentration need to be done to exclude or to verify these hypotheses. In addition, the question for the dominant species at pH 5 has to be answered.

The complexation of Am(III) with acetic and tartaric acid were studied in the same manner. The results on the found complexes, their stoichiometry, and the thermodynamic data are summarized in Tab. 2-11 for acetic acid and in Tab. 2-12 for tartaric acid.

Tab. 2-10: Stability constants at varying temperatures and thermodynamic data of Am(III) complexes with citrate determined by UV-vis (I = 0.1 M $NaClO_4$).

T [°C]	$\log\beta_{110}$	$\log\beta_{120}$	Ref[c)]
25	7.5 ± 0.2[a)]	11.4 ± 0.4[a)]	[HEL2010]
25	6.67 ± 0.63	12.36 ± 0.93	this work
30	7.08 ± 0.11	11.80 ± 0.11	this work
40	7.20 ± 0.10	12.04 ± 0.11	this work
50	7.66 ± 0.26	12.36 ± 0.28	this work
$\Delta_r H$ [kJ mol^{-1}]	41 ± 17	46 ± 12	this work
	11.1 ± 3.1 [b)]	19 ± 3.9 [b)]	[MAT2007]
$\Delta_r S$ [J mol^{-1} K^{-1}]	268 ± 53	376 ± 39	this work
	154 ± 10[b)]	265 ± 13[b)]	[MAT2007]

a) for the analogue Eu(III) complex
b) I=6.6 mol kg-1, pcH 3.6, solvent extraction
c) more references to Ln(III)/An(III) citrate complexes are given in [HEL2010] and [MOM2005]

Tab. 2-11: Stability constants at varying temperatures and thermodynamic data of Am(III) complexes with acetate determined by UV-vis (I = 0.1 M $NaClO_4$).

T [°C]	$\log\beta_{110}$	Ref
25	2.39 ± 0.05	[RAO1987]
25	2.14 ± 0.07	this work
40	2.26 ± 0.07	this work
50	2.30 ± 0.12	this work
$\Delta_r H$ [kJ mol^{-1}]	11 ± 1	this work
	7.1 ± 0.03[a)]	[ZAN2001]
$\Delta_r S$ [J mol^{-1} K^{-1}]	78 ± 3	this work
	66 ± 0.4[a)]	[ZAN2001]

a) determined for the Nd(III) acetate complex at I = 2,2 mol kg^{-1} $NaClO_4$ and 25°C

Tab. 2-12: Stability constants of Am(III)/Eu(III) complexes with tartrate determined by UV-vis at 25°C (I = 0.1 M $NaClO_4$).

ion	$\log\beta_{110}$	$\log\beta_{120}$	Ref
Eu(III)	4.17 ± 0.13	7.27 ± 0.23	this work [ACK2011]
	4.3[a)]	6.0 [a)]	[KUL1986]
Am(III)	3.84 ± 0.10	6.54 ± 0.15	this work [ACK2011]
	4.2 ± 0.06 [b)]	6.84 ± 0.07 [b)]	[RAO1987]

* 0.1 M $NaNo_3$, polarography
** 0.5 M NH_4Cl, solvent extraction

2.3 Conclusions and update of the thermodynamic database

In the present study the complexation behavior of Am(III) and Eu(III) with several small organic acids were studied as function of temperature by means of UV-vis measurements in a LPFC and TRLFS. The stoichiometry of the formed complexes, their stability constants, and thermodynamic data were determined. Several new complexes were identified and thermodynamically characterized, such as the 1:3 Eu(III)-salicylate complex, the 1:1 and 1:2 Am(III)-pyromellitate complexes, and the 1:1 and 1:2 Am(III)-salicylate complexes. Already known complexes were examined by spectrometric methods for the first time, such as the Am(III) complexes with tartaric, citric, acetic, and lactic acid.

Table 2-13 summarizes the obtained complex formation constants and Gibbs free energies of complexation for the 1:1 complexes at an ionic strength of I = 0 (calculated by Davies equation). In any of the studied metal-ligand systems the complexation enthalpies for the 1:1 complexes were found to proceed endothermic with a positive change in the entropy during the complexation. Therefore, the complex formation is driven by entropy. Among the studied acids, citric, pyromellitic, and tartaric acid form complexes with the highest stability. Fig. 2-19 shows a sound correlation between the $\log\beta^0$ of the complexes with the number of carboxylic groups per ligand molecule. The higher the number of the COOH-groups the higher the complex stability. Pyromellitic acid with four carboxylic groups per molecule is an exemption since the complexation of a metal ion by all of the four groups is sterically hindered.

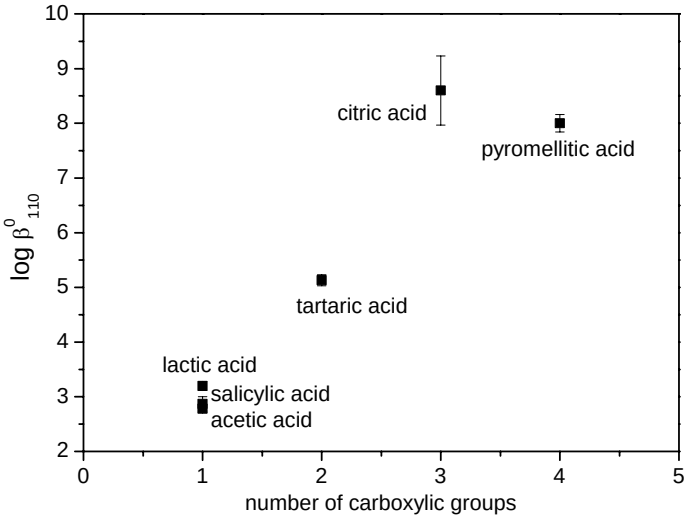

Fig. 2-19: Stability constants $\log\beta^0_{110}$ of 1:1 Am(III)-ligand complexs as function of carboxylic groups number

Complexes with a stoichiometry of higher than 1:1 are typically formed at higher ligand concentrations. For salicylic and lactic acid an excess of the ligand of 0.1 M compared to a metal ion concentration in the micromolar range was necessary to form 1:3 complexes. The thermodynamic data were determined of the found complexes. However, they are considered as less relevant for migration studies.
Pyromellitic acid forms again an interesting exception. This compound exhibits a strong tendency to polymerization in presence of Eu(III). That occurs at higher Eu(III) concentrations (millimolar solutions) already at room temperature. The formed polymeric species are able to form complexes with the present metal ions.

A closer look at the Gibbs free energies of complexation at an ionic strength of I = 0 reveals an interesting detail (Tab. 2-13). The complexes formed between Am(III) and pyromellitic and salicylic acid are slightly more stable than the analogues complexes with Eu(III). If non-aromatic acids are used for complexation, the Eu(III) complexes exhibit a slightly higher stability than those of Am(III) with the same ligands. However, the derived enthalpies and entropies of complexation (Tab. 2-14) exhibit an uncertainty that is too high to attribute the different complex stabilities to an enthalpic or entropic contribution. A further interpretation is useful if more thermodynamic data are available. The next step will be done in the succeeding project with the study of complexation by micro-titration calorimetry.

Tab. 2-13: Stability constants and the Gibbs free energies of 1:1 Am(III)/Eu(III)-ligand complexes at T = 25°C and I = 0

	$\log\beta^0_{110}$		ΔG^0 [kJ·mol^{-1}]	
ligand	Eu(III)	Am(III)	Eu(III)	Am(III)
pyromellitate	7.28 ± 0.06	8.00 ± 0.16	- 41.5 ± 0.3	- 45.6 ± 0.9
salicylate	2.48 ± 0.08	3.20 ± 0.08	- 14.1 ± 0.5	- 18.3 ± 0.5
lactate	3.15 ± 0.13	2.87 ± 0.13	- 18.0 ± 0.7	- 16.4 ± 0.7
acetate	3.46 ± 0.05 [a)]	2.78 ± 0.07	- 19.7 ± 0.3	- 15.9 ± 0.4
tartrate	5.46 ± 0.13	5.13 ± 0.10	- 31.1 ± 0.7	- 29.3 ± 0.6
citrate	9.43 ± 0.20 [b)]	8.60 ± 0.63	- 53.8 ± 1.1	- 49.1 ± 3.6 [c)]

a) calculated from value given in [ZOT200]
b) calculated from value given in [HEL2010]
c) value in very good agreement by the in [MOM2005] selected values ($\log\beta^0_{110}$ = 8.55 ± 0.2 and $\Delta_f G^0$ = - 48,806 ± 1.142)

Tab. 2-14: Enthalpy ΔH^0 and entropy ΔS^0 of Am(III)/Eu(III) ligand 1:1 complexes at 25°C and I = 0

	Eu(III)		Am(III)	
ligand	ΔH^0 [kJ·mol^{-1}]	ΔS^0 [J·mol^{-1}·K^{-1}]	ΔH^0 [kJ·mol^{-1}]	ΔS^0 [J·mol^{-1}·K^{-1}]
pyromellitate	34.7 ± 1.2	256 ± 4	103.2 ± 58.9	496 ± 189
salicylate	2.0 ± 4.9	54 ± 15	--	--
lactate	10.9 ± 9.3	98 ± 29	10.4 ± 6.5	89 ± 20
acetate	--	--	16.5 ± 2.0	109 ± 6
tartrate	--	--	--	--
citrate	--	--	76.8 ± 13.3	424 ± 43

a) ΔH^0 and ΔS^0 values were recalculated from Van't Hoff plots using $\log\beta^0_{110}$ (converted by Davies equation)

3 Eu(III) sorption on Opalinus Clay [SCH2011]

3.1 Experimental

3.1.1 Solutions and reagents

An aerobic OPA sample prepared from the bore core BHE-24/1 from the underground rock laboratory Mont Terri, Switzerland, was used without any purification and other treatments. The average mineral composition of OPA is given in [NAG2002]. The physicochemical properties (N_2-BET surface area, cation exchange capacity) of the OPA sample BHE-24/1 are summarized in [JOS2011].
To simulate the aqueous medium in the OPA rock formation the sorption experiments were carried out in synthetic OPA pore water with a pH of 7.6 and an ionic strength of 0.4 M. The composition of the synthetic OPA pore water was taken from [VAN2003]. In some batch experiments 0.4 M sodium perchlorate as background electrolyte was used to compare the results with published ones in the literature.
Synthetic OPA pore water was prepared under the composition described in [VAN2003]. Chemicals of analytical grade were used without any purification. Different stock solutions (0.01 M, 0.1 M and 1 M) of citric acid (Merck) and tartaric acid (Merck) were prepared by dissolving the according amounts of the solids in deionized water. For sorption experiments with citric acid, ^{14}C-labed citric acid (Hartmann Analytic) were used [SCH2010b]. A carrier free ^{152}Eu solution (Amersham Lifescience) was diluted in the synthetic OPA pore water to get a stock solution with a radiotracer concentration of $5 \cdot 10^{-7}$ M. The ^{152}Eu concentration of this stock solution was verified by γ-spectroscopy (Ortec, detector GMX20P4-70). Aliquots from a $5 \cdot 10^{-3}$ M stock solution of inactive Eu(III) (chapter 2.1.1) were used for TRLFS samples with higher Eu(III) concentrations (10^{-5} M).
Necessary pH adjustments were done with NaOH or $HClO_4$ with an accuracy of 0.05 pH units like described in chapter 2.1.1.

3.1.2 Batch experiments

All sorption experiments were carried out as batch experiments under aerobic conditions ($p(CO_2) = 10^{-3.5}$ atm) in 10 mL polyethylene centrifuge tubes (Sigma Laborzentrifugen GmbH) with 7.5 mL suspensions of OPA in synthetic OPA pore water. The total Eu(III) concentration in each sample was $2 \cdot 10^{-9}$ M. Following series of samples were investigated:

- ♦ Sorption experiments with OPA suspensions at solid-to-liquid ratios from 0.33 $g \cdot L^{-1}$ to 3 $g \cdot L^{-1}$ in dependence on temperature between 15°C and 50°C and in the absence of citrate and tartrate
- ♦ Sorption experiments in the presence of citrate and tartrate in dependence on temperature between 15°C and 50°C with OPA suspensions at a solid-to-liquid ratio of 2 $g \cdot L^{-1}$. The ligand concentration was varied up to $5 \cdot 10^{-3}$ M.
- ♦ pH serie with OPA suspensions at a solid-to-liquid ratio of 2 $g \cdot L^{-1}$ and at 25°C

Comprehensive leaching experiments by Joseph et al. [JOS2011] showed that the equilibrium between the clay and the OPA pore water was reached after 7 days. During this period of time aluminate, silicate, sulfate, carbonate and calcium ions are released due to dissolution processes of some OPA components such as calcite. Thus, in our sorption experiments the OPA was preconditioned at the selected temperature for 5 to 7 days in the synthetic OPA pore water until a stable pH was reached.

After addition of aliquots of ^{152}Eu and tartrate or citrate to the samples the suspensions were equilibrated. During the conditioning of the clay and during the Eu(III) sorption the pH of the samples was readjusted to 7.6 for several times. All samples were permanently stored in a temperature adjustable shaker (HLC, KühlThermomixer) or in an heatable metal block. The Eu(III) sorption was carried out for 7 days to ensure a steady state of the sorption reaction [BAU2005]. After that the samples were centrifuged (3K30H, Sigma Laborzentrifugen GmbH) at the selected temperature and 40,000 g for 1 h. Investigations of the centrifuged clay samples with photon correlation spectroscopy showed supernatants free of particles.
The supernatants, the suspensions, and the acidified suspensions of the sorption samples were analyzed concerning the ^{152}Eu activity by gamma counting (Packard, CobraII) to determine the distribution of Eu(III) between the synthetic OPA pore water and OPA. For that two 1 mL samples of the supernatant of each sorption sample were taken for the analysis. Each sorption sample was then shaken vigorously to get a fine suspension. Two samples of 1 mL of the suspension of each sorption sample were taken for the analysis again. At the end, the remaining part of the suspension was acidified to determine the Eu(III) sorption on the tube wall. Again two samples of 1 mL were taken for the analysis. Around 5 % of the total amount of Eu(III) were found as sorbed on the tube walls.
The distribution coefficient R_d was calculated by Eq. 3-1 [LAU2000],

$$R_{\mathrm{d}} = \frac{c_{\mathrm{in}} - c_{\mathrm{eq}}}{c_{\mathrm{eq}}} \cdot \frac{L}{S} \tag{3-1}$$

(R_d: distribution coefficient [L·kg^{-1}], c_{in}: added Eu(III) concentration [mol·L^{-1}], c_{eq}: equilibrium concentration of Eu(III) [mol·L^{-1}], L·S^{-1}: liquid-to-solid ratio [L·kg^{-1}]).
Another method to determine R_d values is to analyze the experimental sorption isotherms with the Freundlich model in logarithmic form (Eq. 3-2),

$$\log a = \log R + n \log c_{\mathrm{eq}} \tag{3-2}$$

(a: loading of the clay with Eu(III) [mol·kg^{-1}], c_{eq}: equilibrium concentration of Eu(III) [mol·L^{-1}], R: Freundlich coefficient [L·kg^{-1}], n: Freundlich coefficient). For n = 1 log R is equal to log R_d [KLI2007].

3.1.3 Time-resolved laser-induced fluorescence spectroscopy

For the TRLFS studies the total Eu(III) concentration in each sample was 10^{-5} M. Samples with and without OPA were investigated:

- ♦ synthetic OPA pore water samples (without OPA) with citrate and tartrate at 25°C. The ligand concentration was varied up to 10^{-3} M.
- ♦ Sorption samples at 25°C in the presence of citrate and tartrate with OPA suspensions at a solid-to-liquid ratio of 2 g·L^{-1}. The ligand concentration was varied up to 10^{-3} M. The sorption samples were prepared analogue to the batch sorption experiments at 25°C (section 3.1.2).

The TRLFS measurements were performed using a Nd:YAG-OPO laser system (Continuum). Europium luminescence spectra of the supernatants and suspensions were recorded with an optical multichannel analyser consisting of a spectrograph (Oriel MS 257) and an ICCD camera (Andor iStar) with a constant excitation wavelength of 395 nm and pulse energy of 4 mJ. Static and time-resolved spectra were recorded in the wavelength range of 565-650 nm

(1200 line mm^{-1} grating, 0.2 nm resolution, 3000 accumulations) and 440-780 nm (300 line mm^{-1} grating, 0.7 nm resolution, 200 accumulations), respectively. The time-resolved luminescence spectra were recorded with delay times between 10 µs and 100 µs. The samples were transferred into a quartz cuvette, measured with the laser system at 25°C and continuously stirred during the measurements.
The spectra were analyzed with the graphing and data analysis software package Origin™ (version 7.5, OriginLab Corporation). All raw spectra were baseline corrected in the wavelength range between 570 nm and 640 nm. The spectra were normalized to the peak area of the emissions band at 592 nm and the ratios F_1/F_2 of the peak area of the fluorescence emissions band at 592 nm and 616 nm were calculated. The analysis of the time-resolved spectra were carried out like in chapter 2.1.3 described.

3.2 Results and discussion

3.2.1 Influence of Eu(III) concentration

The batch sorption experiments in synthetic pore water were carried out at Eu(III) concentrations ~10^{-9} M, that are realistic for environmental conditions. For the spectroscopic characterisation of the Eu sorption process on OPA with TRLFS higher concentrations (~10^{-5} M) of Eu(III) were necessary, so the Eu(III) speciation in pore water for both concentrations has to be considered (Fig. 3-1)

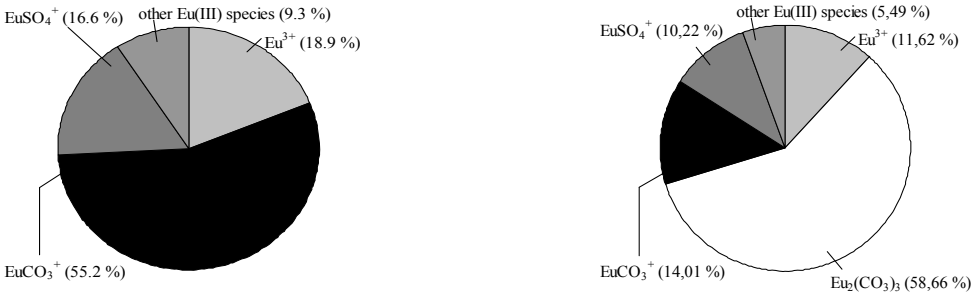

Fig. 3-1: Eu(III) speciation under synthetic pore water conditions. Left: $c_{Eu(III)} = 2 \cdot 10^{-9}$ M. Right: $c_{Eu(III)} = 1 \cdot 10^{-5}$ M. Complexation constants were taken from [HUM2001] and [RAR1985]. Speciation was calculated with the computer code EQ3/6 [WOL1992].

At low concentrations the dominated species is the $EuCO_3^+$, at higher concentration the neutral species $Eu_2(CO_3)_3$ occurs. Precipitations of $Eu_2(CO_3)_{3(s)}$ was not observed neither in synthetic pore water nor in the centrifuged clay samples as verified with photon correlation spectroscopy.
With increasing Eu(III) concentration, the Eu sorption and consequently the R_d values decrease (Fig. 3-2). This decrease may be explained on the one side by a weaker sorption mechanism of the neutral species $Eu_2(CO_3)_3$ and on the other side by high- und low affinity sorption sites. At higher concentration high affinity sorption sites are already occupied and thus low-affinity sites should be embraced, which is resulting in a weaker sorption [FRÖ2011].

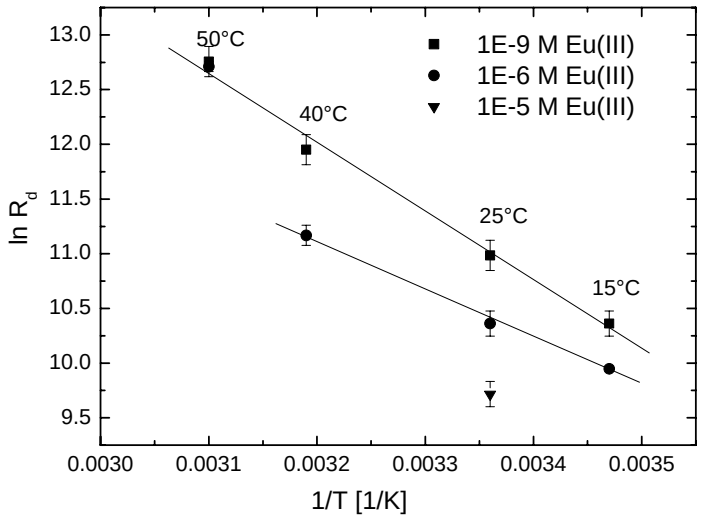

Fig. 3-2: Eu(III) sorption on Opalinus Clay as function of Eu(III) concentration and temperature (synthetic pore water)

3.2.2 Influence of pH

It is well know that the sorption of trivalent lanthanides and actinides on clay minerals depends on pH [BRA2006, BAU2005, HAR2008, RAB2005, FER2008]. Thus, the same behaviour is observed at Eu(III) sorption on OPA in pore water medium. There is a low sorption at pH values smaller than 6. A strong sorption with > 95% Eu(III)sorption occurs at pH values larger than 9. The distribution coefficient R_d increases with increasing pH (Tab. 3-1)

Tab. 3-1: Sorbed Eu(III) and R_d as function of pH, T = 25°C (synthetic pore water)

pH	sorbed Eu [%]	R_d
2.1	< 1	0.37 ± 0.26
3.9	5 ± 1	1.43 ± 0.05
5.1	42 ± 5	2.56 ± 0.05
6.4	70 ± 1	3.14 ± 0.05
7.6	90 ± 5	4.77 ± 0.06
9.4	96 ± 2	5.65 ± 0.05

The pH dependence is accompanied by a change in Eu(III) speciation, as shown by speciation calculations and TRLFS investigations. The different Eu species in pore water solutions interact differently with the OPA surface.
The dominating Eu species between pH 2 and 5 are the positively charged species Eu^{3+}_{aqua} (~47.8%), $EuSO_4^+$(~41.6%), and $EuCl^{2+}$ (~7.7%) The non-specific electrostatic attraction between these species with the negative charged OPA surface [JOS2011b] results in an outer-sphere complex formation. The strong increase of the sorption at pH values larger than 5 goes along with a complex formation between the dominating Eu-carbonato species ($EuCO_3^+$) and the hydroxyl groups of the OPA surface.

Investigations of the pH dependence of Eu-(sorption) speciation with TRLFS were performed to validate this interpretation. The results are summarized in Tab. 3-2.
In synthetic pore water without clay, there are no changes in speciation of Eu(III) until pH 5. The fluorescence properties are nearly constant. The luminescence emission lifetime is in good agreement with that of the Eu(III) aquo ion in water given by (110±5) µs corresponding to 9 water molecules [MOU1999, PLA2003].
At pH 6 the ratio F_1/F_2 of the intensities of the fluorescence emissions band at 592 nm and 616 nm was changed and at pH > 7 the fluorescence emission lifetime increases. The observed enhanced luminescence emission lifetime of 139 ± 2 µs is caused by the formation of Eu(III)-carbonato species, like $EuCO_3^{2+}$, $Eu_2(CO_3)_3$ (see Fig. 3-1). In the literature the luminescence emission lifetimes of $EuCO_3^{2+}$ and $Eu_2(CO_3)_{3(s)}$ are given by 170 ± 10 µs and 234 ± 10 µs, respectively [KIM1994, RUN2000].
The results of the TRLFS investigations correlate with the results of the batch experiments:
Until pH 5 in the suspensions no sorbed species on the OPA can be detected with TRFLS. The analyzed Eu(III) species in the supernatants has nearly the same fluorescence spectra and properties like the species in the synthetic pore water without clay (Tab. 3-2).
At pH ≥ 6 the sorption increases strongly and a sorbed species was observed in the clay suspension and simultaneous, in the supernatant the concentration of not sorbed Eu(III) is deemed to be too low (smaller than 5% of the total Eu(III) concentration) for an analysis with TRLFS. The luminescence emission lifetime of the sorbed Eu(III) species under atmospheric synthetic OPA pore water conditions was determined to be (190 ± 7) µs corresponding to 5.0 ± 0.5 water molecules (Tab. 3-2, Eq. 2-2). So the sorption process of Eu(III) on OPA causes a loss of four water molecules. Thus, an inner sphere surface complex formation between a Eu(III) species, most likely the Eu(III) carbonato species $EuCO_3^{+}$, $Eu_2(CO_3)_3$, and the minerals in OPA under pore water conditions can be postulated.
For comparison, the luminescence emission lifetimes for sorbed Eu(III) species on different minerals are given in Tab. 3-3, which demonstrate a good accordance between this work and previously published values. An(III)/Ln(III) carbonato surface complexes are postulated from modelling calculations [FER2008] and spectroscopic investigations [FER2010, STU2002] at pH > 7

Tab. 3-2: Luminescence emission lifetime (τ), amounts of water molecules in the first coordination shell ($n(H_2O)$) and ratio of transition bands at 592 nm and 616 nm ($^5D_0 \rightarrow {}^7F_1$ to $^5D_0 \rightarrow {}^7F_2 \equiv F_1/F_2$) in (1) synthetic pore water, (2) the supernatant of the sorption sample and (3) the suspension of the sorption sample. Lifetime error: ± 1 σ from repeated experiments

pH	2	3	4	5	6	7.6	9
pore water							
$\tau_{(1)}$ [µs]	116 ± 2	121 ± 6	121 ± 6	109 ± 9	118 ± 2	**139 ± 2**	363 ± 73
$n(H_2O)_{,(1)}$	8.6 ± 0.5	8.2 ± 0.5	8.2 ± 0.5	9.2 ± 0.5	8.4 ± 0.5	**7.1 ± 0.5**	2.3 ± 0.5
F_1/F_2	1.21	1.17	1.14	1.12	1.16	**0.49**	0.41
species	Eu^{3+}_{aquo} (~ 47.8%), $EuSO_4^+$ (~ 41.6%), $EuCl^{2+}$ (~ 7.7%)					$EuCO_3^{2+}$ (14%), $Eu_2(CO_3)_3$ (59 %)	Eu-carbonates hydroxides
supernatant							
$\tau_{(2)}$ [µs]	121 ± 4	106 ± 5	106 ± 5	117 ± 10	115 ± 6	**n.d.**	n.d.
$n(H_2O)_{,(2)}$	7.5 ± 0.5	9.5 ± 0.5	9.5 ± 0.5	8.5 ± 0.5	8.7 ± 0.5	**n.d.**	n.d.
F_1/F_2	1.10	1.05	0.98	0.89	0.96	**n.d.**	n.d.
species	Eu^{3+}_{aquo} (~ 47.8%), $EuSO_4^+$ (~ 41.6%), $EuCl^{2+}$ (~ 7.7%)						
suspension							
$\tau_{(3)}$ [µs]	n.d.	n.d.	n.d.	n.d.	112 ± 9	**190 ± 7**	849 ± 23
$n(H_2O)_{,(3)}$	n.d.	n.d.	n.d.	n.d.	8.9 ± 0.5	**5.0 ± 0.5**	0.6 ± 0.5
F_1/F_2	n.d.	n.d.	n.d.	n.d.	0.30	**0.34**	0.42
species	--	--	--		Eu(III)carbonato surface complex		

n.d. not detectable

Tab. 3-3: Luminescence emission lifetimes of sorbed Eu(III) species under atmospheric conditions

system	t [µs]	Ref.
Eu(III), OPA, pH 7.6	190 ± 7	this work
Eu(III), OPA, pH 7.6 (in presence of citric or tartaric acid)	201 ± 9	this work (averaged)
Eu(III), γ-Al_2O_3, pH 7	239	[RAB2000]
Eu(III), SiO_2, pH 8	215	[PAT2007]
Eu(III), smectite, pH 7.9	180	[BAU2005]
Eu(III), gibbsite, pH 6.9	220 ± 30	[TER2006]
Eu(III), smectite, pH 7.1	333 ± 20	[STU2001]

3.2.3 Influence of temperature

These batch experiments were performed under synthetic pore water conditions at pH 7.6. Similar experiments which are described in literature were done in sodium perchlorate medium. Hence for comparisons with literature values several additional batch experiments were carried out in $NaClO_4$ solution with the same ionic strength like the pore water. Averaged distribution coefficients R_d for the different solid-to-liquid ratios calculated at different temperatures as well as selected literature values are compared in Table 3-4.

Tab. 3-4: Log R_d values for the sorption of some radionuclides on OPA and other clay minerals. R_d [$l \cdot kg^{-1}$] Error: $\pm 1\sigma$ from repeated experiments

T [°C]	system	log R_d calculated by		reference
		Eq. 3-1	Eq. 3-2 ($n = 1$)	
15	Eu(III), OPA, pore water, pH 7.6	4.50 ± 0.05	4.47 ± 0.01	this work
25	Eu(III), OPA, pore water, pH 7.6	4.77 ± 0.06	4.79 ± 0.01	this work
40	Eu(III), OPA, pore water, pH 7.6	5.19 ± 0.06	5.16 ± 0.02	this work
50	Eu(III), OPA, pore water, pH 7.6	5.54 ± 0.06	5.51 ± 0.01	this work
15	Eu(III), OPA, 0.4 M $NaClO_4$, pH 7.6	5.38 ± 0,10	n.e.	this work
25	Eu(III), OPA, 0.4 M $NaClO_4$, pH 7.6	5.53 ± 0,15	n.e.	this work
40	Eu(III), OPA, 0.4 M $NaClO_4$, pH 7.6	5.62 ± 0,31	n.e.	this work
50	Eu(III), OPA, 0.4 M $NaClO_4$, pH 7.6	5.82 ± 0,28	n.e.	this work
25	Eu(III), OPA, pore water, pH 7.2	4.78		[BRA2003]
25	Eu(III), OPA, 0.1 M $NaClO_4$, pH 7.6	~ 4.6		[HAR2008]
25	Am(III), OPA, pore water, pH 7.6	4.48		[BRA2003]
25	Np(V), OPA, saturated calcite solution, pH 8.2	2.15		[FRÖ2011]
25	Np(V), OPA, pore water, pH 7.6	1.34		[BAU2005]
25	U(VI), OPA, pore water, pH 7.6	1.48		[AMA2007]
25	U(VI), OPA, pore water, pH 7.6	1.35		[JOS2011]
25	Eu(III), montmorillonite, 0.5 M $NaClO_4$, pH 7.6	~ 4.8		[TER2006]
40	Eu(III), montmorillonite, 0.5 M $NaClO_4$, pH 7.6	~ 5.2		[TER2006]
25	Eu(III), kaolinite, 0.5 M $NaClO_4$, pH 7.6	~ 3.1		[TER2006]
40	Eu(III), kaolinite, 0.5 M $NaClO_4$, pH 7.6	~ 4.1		[TER2006]

n.e. not estimated

The sorption isotherms shown in Fig. 3-3 are parallel shifted to lower Eu(III) equilibrium concentrations with increasing temperature. Fitting by the Freundlich formalism (Eq. 3-2) with a fixed slope of 1 yields to R_d values which are consistent to the R_d values calculated by Eq. 3-1 (Tab. 3-4)

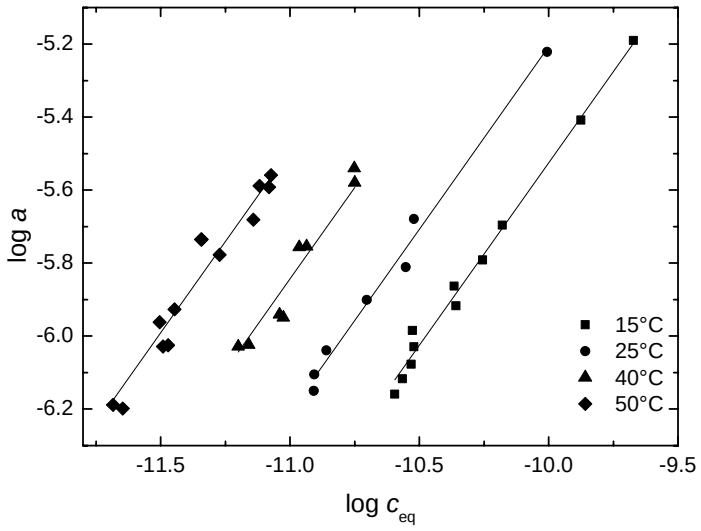

Fig. 3-3: Sorption isotherms at different temperatures for the Eu(III) sorption on OPA in synthetic pore water fitted with the Freundlich model ($n = 1$); $c_{Eu(III)} = 2 \cdot 10^{-9}$ M

The free fitting of the sorption isotherms leads independently to slopes of the isotherms of about 1.

The R_d values determined in synthetic pore water are lower than the values determined in sodium perchlorate solutions (Tab. 3-4, Fig. 3-4). A possible explanation for this fact might a competition between the cations in the synthetic pore water and Eu(III) cations for the sorption sites of the OPA. Generally, the determined R_d values are in good agreement with the literature data for comparable conditions and analogous systems (Tab. 3-4).

The sorption of Eu(III) on OPA is an endothermic surface reaction in synthetic pore water as well as in $NaClO_4$ medium. From the ln R_d versus T^{-1} plot (Fig. 3-4) a sorption enthalpy ΔH_{sorb} of (52 ± 4) kJ·mol^{-1} was determined for synthetic OPA pore water and a value of (21 ± 13) kJ·mol^{-1} for 0.4 M $NaClO_4$. The sorption entropies ΔS_{sorb} were calculated as (267 ± 12) J·K^{-1}·mol^{-1} and (176 ± 44) J·K^{-1}·mol^{-1}, respectively.

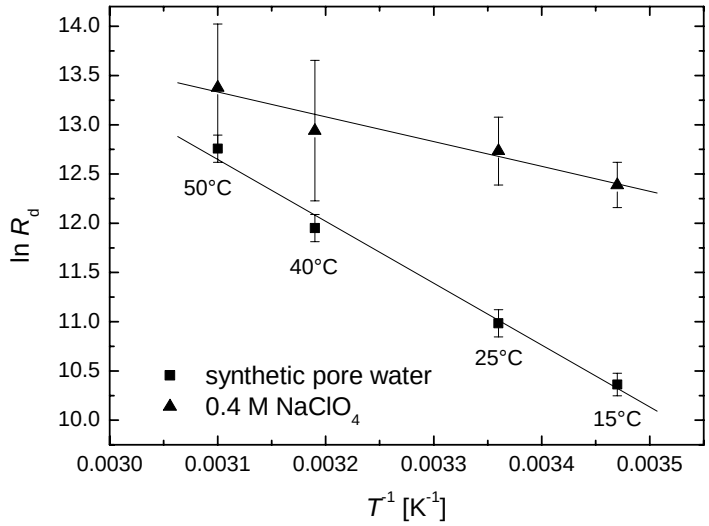

Fig. 3-4: R_d of the Eu(III) sorption on OPA as a function of the temperature. Error bar: ± 1σ from repeated experiments

The calculated value for ΔH_{sorb} in pore water confirms the ΔH_{sorb} value of (47 ± 8) kJ·mol^{-1}, which was determined in [SCH2010]. Hence, the reproducibility of the sorption experiments is ensured. Tertre et al. [TER2005] determined a comparable ΔH_{sorb} value of (39 ± 15) kJ·mol^{-1} for the system Eu(III)/montmorillonite in 0.025 M $NaClO_4$. In our investigation the temperature dependent Eu(III) sorption in pore water medium is higher pronounced than in the sodium perchlorate medium.

The increasing sorption with rising temperature could be explained with an increase of the negative surface charge [BRA1994, TER2006b, ROZ2009]. This induces more binding sites for positively charged Eu(III) species, like $EuCO_3^+$, which is the dominant Eu(III) species under synthetic OPA pore water conditions at very low Eu(III) concentrations (see Fig. 3-1). An another possible explanation for the observed sorption behaviour could be that changes in the hydration shell of Eu(III) lead to an enforced connection to the clay surface. Such changes in the hydration shell of metal ions with rising temperature are reported for instance in [LIN2005] and [LIM2010].

High R_d values, and the pronounced temperature dependence of R_d for the Eu(III) sorption on OPA under synthetic OPA pore water conditions indicate an inner sphere surface complex formation. An outer sphere surface complex, which is a non-specific electrostatic interaction, would be characterized by small R_d values and weak temperature dependence [TER2005]. The inner sphere surface complex formation takes place between the hydroxyl groups located on the mineral surfaces [HAR2008, BAU2005, TER2005] and the Eu(III) species. The TRLFS results (see chapter 3.2.2) indicate, that the $EuCO_3^+$ species is involved in the sorption process.

3.2.4 Influence of small organic ligands

In the presence of small organic ligands like citrate or tartrate the Eu(III) sorption decreases with increasing ligand concentration at all investigated temperatures duo to a complex formation between Eu(III) and the ligands in solutions (Fig. 3-5).
A significant decrease of the Eu(III) retention on OPA at a fixed temperature could be observed for a tartrate concentration above 10^{-4} M (Fig. 3-5 left) or a citrate concentration of 10^{-5} M (Fig. 3-5 right). Tab. 3-5 shows the decrease of the Eu(III) retention at the highest investigated ligand concentration ($5 \cdot 10^{-3}$ M) for different temperatures.

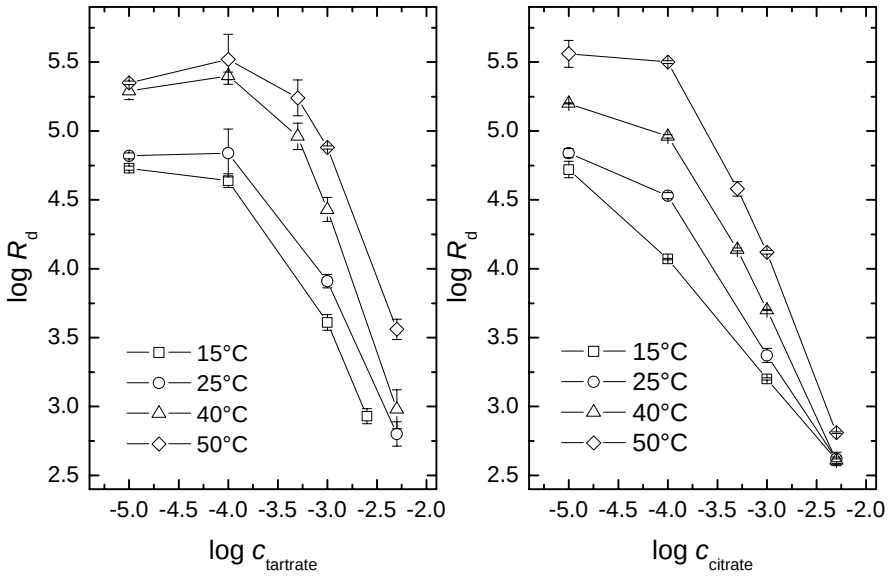

Fig. 3-5: Log R_d of the Eu(III) sorption on OPA in dependence on the ligand concentration and temperature. Left: tartrate, $c_{Eu(III)} = 2 \cdot 10^{-9}$ M, $S \cdot L^{-1} = 2$ g·L^{-1}. Right: citrate, $c_{Eu(III)} = 2 \cdot 10^{-9}$ M, $S \cdot L^{-1} = 2$ g·L^{-1}. Error bar: $\pm 1\sigma$ from repeated experiments

Tab. 3-5 Comparison of the influence of tartrate and citrate on the Eu(III) sorption on OPA;$_d$ $c_{Eu(III)} = 2 \cdot 10^{-9}$ M, $S \cdot L^{-1} = 2$ g·L^{-1}

	Eu(III) sorption on OPA [%]		
T [°C]	in the absence of the ligand	at $5 \cdot 10^{-3}$ M tartrate	at $5 \cdot 10^{-3}$ M citrate
15	95	50	44
25	95	53	44
40	95	62	43
50	95	79	56

Citrate causes a greater lowering of the Eu(III) retention than tartrate. Hence, the influence of citrate and tartrate correlates with the complex stability as the formation constants log β_{120} of the 1:2 complex, which is assumed to formed at this pH value: Eu-tartrate: 7.3 ± 0.5 [ACK2011, chapter 2.2.6], Eu-citrate: 11.4 ± 0.4 [HEL2011] for I = 0.1 M $NaClO_4$.
The temperature influence in the presence of citrate or tartrate is the same as in the absence of these ligands. With rising temperature the sorption of Eu(III) increases (Fig. 3-5). The most pronounced effect is observed at small ligand concentrations. Hence, the complex formation in solution exceeds the temperature influence on the Eu(III) sorption on OPA.

The complex formation between Eu(III) and citrate/tartrate was confirmed by TRLFS experiments at 25°C. Starting from a citric acid concentration of $5 \cdot 10^{-5}$ M and from a tartaric acid concentration of $1 \cdot 10^{-4}$ M changes in the TRLFS spectra (Fig. 3-6 (1a) and (1b)) and luminescence emission lifetimes (Tab. 3-7) of Eu(III) are observed for the pore water samples (without OPA). At these ligand concentrations detectable amounts of the Eu(III) tartrate or citrate complexes occur in solution. From this spectroscopic result no impact on the Eu(III) sorption until these critical ligand concentrations was assumed for the subsequent TRLFS experiments like the following results showed.

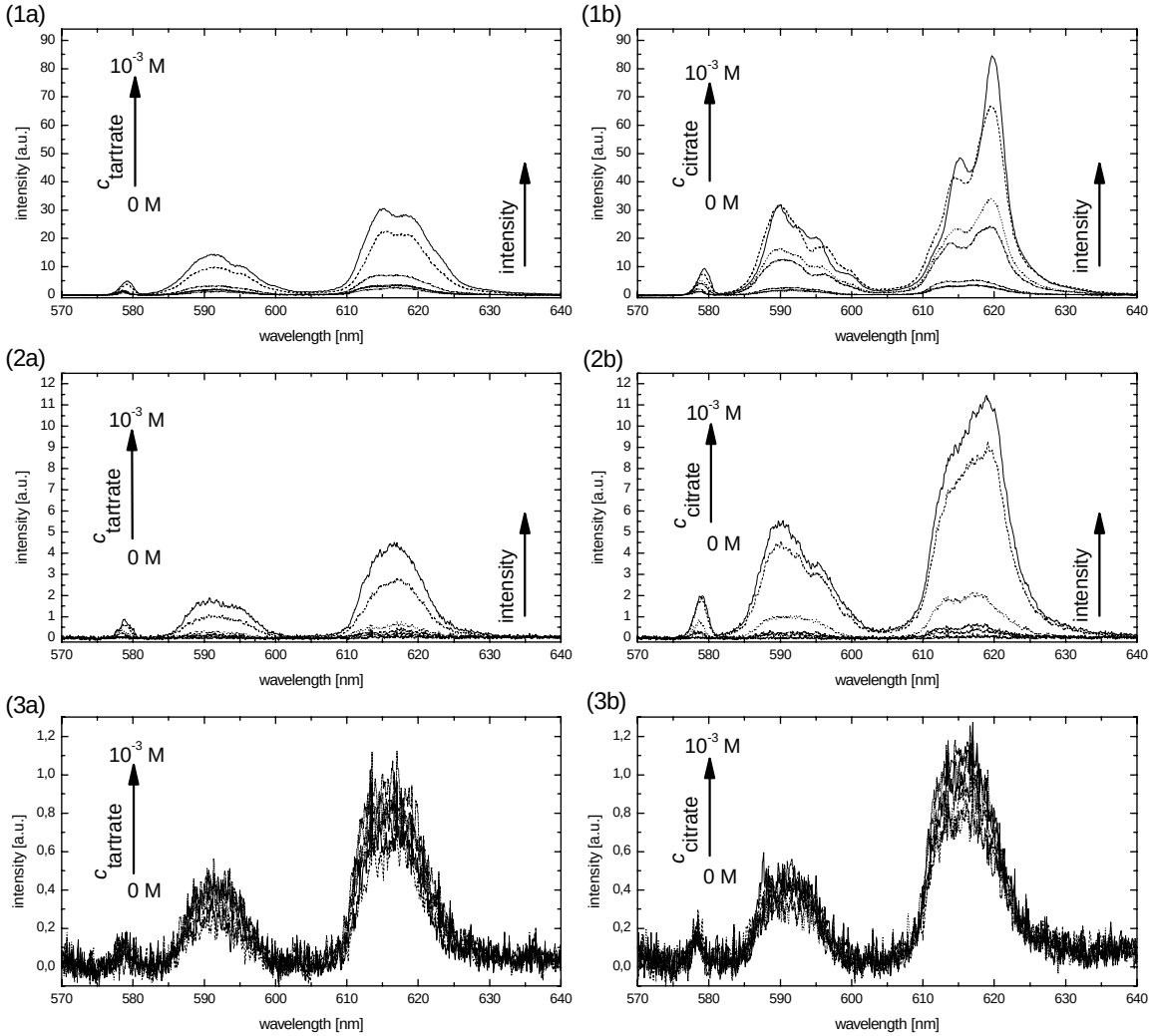

Fig. 3-6: Luminescence spectra of Eu(III) ($c_{Eu(III)}$ = 10^{-5} M) in **(1)** the synthetic OPA pore water, **(2)** the supernatant of the sorption sample and **(3)** the suspension of the sorption sample ($S \cdot L^{-1}$ = 2 g·L^{-1}), in dependence on (a) the tartrate concentration and (b) the citrate concentration

Fig. 3-6 (3a and 3b), shows the Eu(III) luminescence spectra of the supernatants of the sorption samples in dependence on the citrate and tartrate concentration. Until a tartrate concentration of 10^{-4} M and a citrate concentration of 10^{-5} M only small amounts of Eu(III), which are assigned to unsorbed Eu(III), were detected – but not enough to determine luminescence emission lifetimes (Tab. 3-7). From a tartrate concentration of 10^{-4} M and a citrate concentration of 10^{-5} M changes in the TRLFS spectra and luminescence emission lifetimes could be determined again (Tab 3-7).

Combining the results of the spectroscopic investigations of the pore water samples and the supernatants with the results of the batch sorption experiments it can be concluded that the Eu(III) desorption from OPA correlates with the occurrence of significant amounts of the Eu(III) tartrate or citrate complexes in solution.

The luminescence spectra and the luminescence emission lifetimes of the suspensions differ between 0 M and 10^{-3} M tartrate and citrate marginally (Fig. 3-6, (3a) and (3b), Tab. 3-7). From this result it can be assumed that the sorbed Eu(III) species undergo no structural changes in the presence of the used ligands. That means, that tartrate and citrate are not involved in the formation of the Eu(III) surface complex, contrary to e.g. humic acids, which could form coatings on minerals or ternary complexes with metal ions [MUR1992, STE2011]. The metal ion binding to the mineral surface could then occur due to the humic acid coating in dependence on pH and ionic strength [FAI1995, WAN2004, TAK1998] or due to the sorption of the mentioned ternary complexes. Tartrate and citrate play a role in solution as complexing agents and, therefore, as desorbing agents exclusively. The reason for that is a weak outer sphere sorption of small organic ligands, like citrate, on minerals, which is described elsewhere [ANG2006, KUB1999, LAC2003]. In this work a weak (< 15 % at $1 \cdot 10^{-3}$ mol·l^{-1}) and nearly temperature independently ($\Delta H_{sorb} \sim -7 \pm 2$ kJ·mol^{-1}) sorption of citric acid on OPA was determined in batch sorption experiments with ^{14}C-labelled citric acid in absence of Eu(III) [SCH2010b].
The luminescence emission lifetime of the sorbed Eu(III) species averaged over all suspension spectra in the absence as well as in the presence of the organic ligands was determined with (201 ± 9) µs and agrees with the literature values for sorbed Eu(III) species under atmospheric conditions (Tab. 3-3). This luminescence emission lifetime corresponds to the loss of 4 water molecules in comparison to the Eu(III) aquo ion with 9 water molecules.

Tab. 3-7: Luminescence emission lifetimes (τ) and amounts of water molecules in the first coordination shell ($n(H_2O)$) of Eu(III) in **(1)** the synthetic OPA porewater without clay, **(2)** the supernatant of the sorption sample and **(3)** the suspension of the sorption sample, in dependence on the tartrate and citrate concentration. Lifetime error: ± σ from repeated experiments

$c_{tartrate}$ [mol/l]	0	$5 \cdot 10^{-6}$	$1 \cdot 10^{-5}$	$5 \cdot 10^{-5}$	$1 \cdot 10^{-4}$	$5 \cdot 10^{-4}$	$1 \cdot 10^{-3}$
$\tau_{(1)}$ [µs]	139 ± 2	146 ± 2	129 ± 1	149 ± 2	199 ± 2	381 ± 3	423 ± 3
$n(H_2O)_{,(1)}$	7.1 ± 0.5	6.7 ± 0.5	7.7 ± 0.5	6.6 ± 0.5	4.7 ± 0.5	2.2 ± 0.5	1.9 ± 0.5
$\tau_{(2)}$ [µs]	--	--	--	--	157 ± 6	303 ± 4	360 ± 10
$n(H_2O)_{,(2)}$	--	--	--	--	6.2 ± 0.5	2.9 ± 0.5	2.4 ± 0.5
$\tau_{(3)}$ [µs]	190 ± 7	205 ± 9	198 ± 7	181 ± 6	181 ± 8	204 ± 12	208 ± 11
$n(H_2O)_{,(3)}$	5.0 ± 0.5	4.6 ± 0.5	4.8 ± 0.5	5.3 ± 0.5	5.3 ± 0.5	4.6 ± 0.5	4.5 ± 0.5

Continue **Tab. 3-7**

$c_{citrate}$ [mol/l]	0	$5\cdot10^{-6}$	$1\cdot10^{-5}$	$5\cdot10^{-5}$	$1\cdot10^{-4}$	$5\cdot10^{-4}$	$1\cdot10^{-3}$
$\tau_{(1)}$ [µs]	139 ± 2	131 ± 3	151 ± 3	316 ± 6	469 ± 6	556 ± 4	539 ± 4
$n(H_2O)_{,(1)}$	7.1 ± 0.5	7.5 ± 0.5	6.5 ± 0.5	2.8 ± 0.5	1.7 ± 0.5	1.3 ± 0.5	1.4 ± 0.5
$\tau_{(2)}$ [µs]	--	--	130 ± 7	148 ± 5	179 ± 3	345 ± 6	391 ± 4
$n(H_2O)_{,(2)}$	--	--	7.6 ± 0.5	6.6 ± 0.5	5.4 ± 0.5	2.5 ± 0.5	2.1 ± 0.5
$\tau_{(3)}$ [µs]	190 ± 7	206 ± 8	204 ± 8	200 ± 10	216 ± 10	227 ± 9	212 ± 7
$n(H_2O)_{,(3)}$	5.0 ± 0.5	4.6 ± 0.5	4.6 ± 0.5	4.7 ± 0.5	4.3 ± 0.5	4.1 ± 0.5	4.4 ± 0.5

3.3. Conclusions

The Eu(III) sorption on OPA was investigated with batch sorption experiments and TRLFS. The sorption is characterized by a very strong sorption to the clay surface in comparison to the U(VI) and Np(V) sorption in the same system (Tab. 3-4). The luminescence emission lifetimes of determined Eu(III) surface species are similar to the luminescence emission lifetimes of surface species on single mineral phases. Thus, with respect to the literature, e.g. [STU2002], and the TRLFS results of this work a ternary OPA/Eu(III)/carbonato inner sphere surface complex can be assumed. A possible surface species for the investigated Eu(III)/OPA/synthetic OPA pore water system could be $\equiv X\text{-}OEuCO_3^{\pm0}$ [FER2008]. However another possible structure of the Eu(III) surface species might be deduced from the TRLFS results: The Eu(III) species could be coordinated bidentate to the hydroxyl surfaces and bidentate to CO_3^{2-} to the structure $(\equiv X\text{-}O)_2EuCO_3^-$. Eu(III) could also be incorporated into the bulk structure of OPA. Both, the bidentate connection of Eu(III) to the mineral surface and the possible incorporation would explain the strong sorption of Eu(III) and trivalent actinides on OPA. At this point EXAFS investigations could provide specified information about the structure of this Eu(III) inner sphere surface complex.

It could be shown that the Eu(III) sorption increases with rising temperature. The sorption enthalpy was calculated with around 50 $kJ\cdot mol^{-1}$. This work makes a contribution to close the gap in the thermodynamic sorption data up to 50°C. However, more temperature related speciation and sorption data (> 50°C) have to be measured for safety assessments and modelling of the radionuclide migration.

Small organic ligands, like citrate and tartrate influence the Eu(III) sorption on OPA. With increasing ligand concentration the Eu(III) sorption decreases. It can be concluded that the stability constant of the Eu(III) inner sphere surface complex is weaker than the complexes between Eu(III) and citrate or tartrate in solution. Therefore, these small organic ligands are able to increase the mobilization of trivalent lanthanides and, most likely, actinides. However regarding to the very low NOM content, which is found in the OPA formation of Mont Terri, Switzerland, the organic matter should influence the Ln(III)/An(III) sorption on OPA only marginally. Thus, in this OPA formation the sorption should be the dominant physiochemical process in addition to diffusion processes.

The investigations in this work proved that argillaceous rock formations, like Opalinus Clay are efficient materials to sorb trivalent lanthanides and, most likely, actinides, which makes it interesting as potential host rocks and backfill materials for nuclear waste repositories.

4 References

[AMA2007] Amayri, S., Buda, R. A., Fröhlich, D., Heinrich, J., Klimach, T., Kratz, J. V., Reich, T., Trautmann, N., Wunderlich, T.: Sorption of Actinides (Th, U, Np, Pu, Am) on Opalinus Clay in Synthetic Porewater. Jahresberichte, Institut für Kernchemie, Universität Mainz (2007)

[ACK2011] Acker, M., Müller, M., Barkleit, A., Taut, S.: UV-vis study of complexation of trivalent Am, Eu, and Nd by tartaric acid at low metal concentrations. HZDR-IRC Annual Report 2010, Helmholtz-Zentrum Dresden-Rossendorf (2011)

[ANG2006] Angove, M. J., Wells, J. D., Johnson, B. B.: Influence of temperature on the adsorption of mellitic acid onto kaolinite. Langmuir 22, 4208 (2006)

[AOY2004] Aoyagi, N., Toraishi, T., Geipel, G., Hotokezaka, H., Nagasaki, S., Tanaka, S.: Fluorescence characteristics of complex formation of europium(III)-salicylate. Radiochim. Acta. 92, 589-593 (2004)

[ARE1980] Arena, G., Cali, R., Grasso, M., Musumeci, S., Sammartano, S., Rigano, C.: Formation of proton and alkali-metal complexes with ligands of biological interest in aqueous-solution .1. Potentiometric and calorimetric investigation of h+ and na+ complexes with citrate, tartrate and malate. Thermochim. Acta. 36, 329-342 (1980)

[BAR1995] Barbanel, Y. A.: Nephelauxetic Effect in the Optical Spectra of Americium(III). Radiochemistry 38, 27 (1996)

[BAR1998] Barone, V., Cossi, M.: Quantum calculation of molecular energies and energy gradients in solution by a conductor solvent model. J. Phys. Chem. A. 102, 1995-2001 (1998)

[BAR2011a] Barkleit, A., Geipel, G., Acker, M., Taut, S., Bernhard, G.: First fluorescence spectroscopic investigation of Am(III) complexation with an organic carboxylic ligand, pyromellitic acid. Spectrochim. Acta A 78, 549 (2011)

[BAR2011b] Barkleit, A., Tsushima, S., Savchuk, O., Philipp, J., Heim, K., Acker, M., Taut, S., Fahmy, K.: Eu(3+)-Mediated Polymerization of Benzenetetracarboxylic Acid Studied by Spectroscopy, Temperature-Dependent Calorimetry, and Density Functional Theory. Inorg. Chem. 50, 5451-5459 (2011)

[BAU2005] Bauer, A., Rabung, T., Claret, F., Schäfer, T., Buckau, G., Fanghänel, T.: Influence of temperature on sorption of europium onto smectite: The role of organic contaminents. Applied Clay Science 30, 1 (2005)

[BEI1994] Beitz, J. V.: F-state luminescence of trivalent lanthanide and actinide ions in solution. J. Alloys Compd. 207, 41 (1994)

[BIN2005] Binstead, R. A., Zuberbühler, A. D., Jung, B., SPECFIT Global Analysis System, Version 3.040, Spectrum Software Associates, Marlborough, MA, US 2005

[BON1964] Bondi, A.: Van der waals volumes + radii. J. Phys. Chem. 68, 441 (1964)

[BRA1994] Brady, P. V.: Alumina surface chemistry at 25, 40, and 60°C. Geochim. Cosmochim. Acta 58, 1213 (1994)

[BRA2003] Bradbury, M. H., Baeyens, B.: Far-Field Sorption Data Bases for Performance Assessment of a High-Level Radioactive Waste Repository in an Undisturbed Opalinus Clay Host Rock. Technischer Bericht NTB 02-19, NAGRA Nationale Genossenschaft für die Lagerung radioaktiver Abfälle (2003).

[BRA2006] Bradbury, M. H., Baeyens, B.: Modelling sorption data für the actinides Am(III), Np(V) and Pa(V). Radiochimica Acta 94, 619 (2006)

[CAO2009] Cao, Z. J., Balasubramanian, K., Calvert, M. G., Nitsche, H.: Solvation Effects on Isomeric Preferences of Curium(III) Complexes with Multidentate phosphonopropionic Acid Ligands: CmH(2)PPA(2+) and CmHPPA(+) Complexes. Inorg. Chem. 48, 9700 (2009)

[CAR1964] Carnall, W. T., Wybourne, B. G.: Electronic energy levels of the lighter actinides: U^{3+}, Np^{3+}, Pu^{3+}, Am^{3+}, and Cm^{3+}. J. of Chem. Phys. 40, 3428 (1964)

[CAR1968] Caranall, W. T., Fields, R. P., Ranjak, K.: Spectral Intensities of the Trivalent Lanthanides and Actinides in Solution. II. Pm^{3+}, Sm^{3+}, Eu^{3+}, Gd^{3+}, Tb^{3+}, Dy^{3+}, and Ho^{3+}, J. of Chem. Phys. 49, 4412 (1968)

[CHO1994] Choppin, G. R., Rizkalla, E. N., Elansi, T. A., Dadgar, A.: Complexation Thermodynamics of Lanthanide Ions by Benzenepolycarboxylate Ligands. J. Coord. Chem. 31, 297 (1994)

[DER1999] De Robertis, A., De Stefano, C., Foti, C.: Medium effects on the protonation of carboxylic acids at different temperatures. J. Chem. Eng. Data. 44, 262 (1999)

[DIN2008] DIN 32645, Chemical analysis - Decision limit, detection limit and determination limit under repeatable conditions - Terms, methods, evaluation. Beuth Verlag, (2008)

[DOL1989] Dolg, M., Stoll, H., Savin, A., Preuss, H.: Energy-adjusted pseudopotentials for the rare-earth elements. Theor. Chim. Acta. 75, 173 (1989)

[EBE1972] Eberle, S. H., Moattar, F.: Die Komplexe des Am(III) mit Zitronensaeure. Inorg. Nucl. Chem. Letters 8, 265 (1972)

[FAI1995] Fairhurst, A. J., Warwick, P., Richardson, S.: The influence of humic acid on the adsorption of europium onto inorganic colloids as a function of pH. Colloids Surfaces A: Physicochem. Eng. Aspects 99, 187 (1995)

[FER2008] Fernandes, M. M., Baeyens, B., Bradbury, M. H.: The influence of carbonate complexation on lanthanide/actinide sorption on montmorillonite, Radiochimica Acta 96, 691 (2008)

[FER2010] Fernandes, M. M., Stumpf, T., Baeyens, B., Walther, C., Bradbury, M. H.: Spectroscopic Identification of Ternary Cm-Carbonate Surface Complexes. Environ. Sci. Technol. 44, 921 (2010).

[FRI2004] Frisch, M. J., Trucks, G. W., Schlegel, H. B., Scuseria, G. E., Robb, M. A., Cheeseman, J. R., Montgomery, J., J. A., Vreven, T. K., K. N., Burant, J. C., Millam, J. M., Iyengar, S. S., Tomasi, J., Barone, V., Mennucci, B., Cossi, M., Scalmani, G., Rega, N., Petersson, G. A., Nakatsuji, H., Hada, M., Ehara, M., Toyota, K., Fukuda, R., Hasegawa, J., Ishida, M., Nakajima, T., Honda, Y., Kitao, O., Nakai, H., Klene, M., Li, X., Knox, J. E., Hratchian, H. P., Cross, J. B., Bakken, V., Adamo, C., Jaramillo, J., Gomperts, R., Stratmann, R. E., Yazyev, O., Austin, A. J., Cammi, R., Pomelli, C., Ochterski, J. W., Ayala, P. Y., Morokuma, K., Voth, G. A., Salvador, P., Dannenberg, J. J., Zakrzewski, V. G., Dapprich, S., Daniels, A. D., Strain, M. C., Farkas, O., Malick, D. K., Rabuck, A. D., Raghavachari, K., Foresman, J. B., Ortiz, J. V., Cui, Q., Baboul, A. G., Clifford, S., Cioslowski, J., Stefanov, B. B., Liu, G., Liashenko, A., Piskorz, P., Komaromi, I., Martin, R. L., Fox, D. J., Keith, T., Al-Laham, M. A., Peng, C. Y., Nanayakkara, A., Challacombe, M., Gill, P. M. W., Johnson, B., Chen, W., Wong, M. W., Gonzalez, C., Pople, J. A.: Gaussian 03, Revision D.01. Gaussian, Inc., Wallingford CT (2004).

[FRÖ2011] Fröhlich, D. R., Amayri, S., Drebert, J., Reich, T.: Sorption of neptunium(V) on Opalinud Clay under aerobic/anaerobic conditions. Radiochimica Acta 99, 1 (2011)

[GLA2005] Glaus, M. A., Baeyens, B., Lauber, M., Rabung, T., Van Loon, L. R.: Influence of water-extractable organic matter from Opalinus Clay on the sorption and speciation of Ni(II), Eu(III) and Th(IV). Appl. Geochem. 20, 443 (2005).

[GON1987] Goncalves, M. L. S., Mota, A. M.: Complexes of vanadyl and uranyl ions with the chelating groups of humic matter. Talanta. 34, 839 (1987)

[GUI2003] Guillaumont, R., Fanghänel, T., Fuger, J., Grenthe, I., Neck, V., Palmer, D. A., Rand, M. H.:Update on the Chemical Thermodynamics of Uranium, Neptunium, Plutonium, Americium and Technetium. Amsterdam: Elsevier, 2003.

[HAR2008] Hartmann, E., Geckeis, H., Rabung, T., Lützenkirchen, J., Fanghänel, T.: Sorption of radionuclides onto natural clay rocks, Radiochimica Acta 96, 699 (2008)

[HAS1989] Hasegawa, Y., Morita, Y., Hase, M., Nagata, M.: Complexation of lanthanoid(III) with substituted benzoic or phenylacetic acids and extraction of these acids. Bull. Chem. Soc. Jpn. 62, 1486 (1989)

[HAS1990] Hasegawa, Y., Yamazaki, N., Usui, S., Choppin, G. R.: Effects of phenyl groups on thermodynamic parameters of lanthanoid(III) complexation with aromatic carboxylic-acids. Bull. Chem. Soc. Jpn. 63, 2169 (1990a)

[HEL2010] Heller, A.: Spektroskopische Untersuchungen zur Komplexbildung von Cm(III) und Eu(III) mit organischen Modellliganden sowie ihrer chemischen Bindungsform in menschlichem Urin (in vitro).TU Dresden (2011)

[HEL2011] Heller, A., Barkleit, A., Foerstendorf, H., Bernhard, G.: Luminescence and absorption spectroscopic study on the complexation of europium(III) with citric acid. HZDR-IRC Annual Report 2010, Helmholtz-Zentrum Dresden-Rossendorf (2011)

[HOR1979] Horrocks, W. D., Sudnick, D. R.: Lanthanide ion probes of structure in biology - laser-induced luminescence decay constants provide a direct measure of the number of metal-coordinated water-molecules. J. Am. Chem. Soc. 101, 334 (1979)

[HOT2007] Hoth, P., Wirth, H., Reinhold, K., Bräuer, V., Krull, P., Feldrappe, H.: Endlagerung radioaktiver Abfälle in tiefen geologischen Formationen Deutschlands. Untersuchung und Bewertung von Tongesteinsformationen. Bundesanstalt für Geowissenschaften und Rohstoffe BGR (2007).

[HUB1974] Hubert, S., Hussonnois, M., Brillard, L., Goby, G., Guillaumont, R.: Determination simultanee de constants de formation de complexes citrique de l`Americium, du Curium, du Californium, de l`Einsteinium et du Fermium. J. Inorg. Nucl. Chem. 36, 2361 (1974)

[HUM2002] Hummel, W., Berner, U., Curti, E., Pearson, F. J., Thoenen, T.: Nagra / PSI Chemical Thermodynamic Data Base 01/01. Technischer Bericht 02-16, NAGRA National Cooperative for the Disposal of Radioactive Waste (2002).

[HUM2002b] Hummel, W., Berner, U., Curti, E., Pearson, F. J., Thoenen, T.: Nagra/PSI chemical thermodynamic data base 01/01. Radiochim. Acta. 90, 805 (2002)

[INF2008] Infante, C. M. C.; Rocha, F. R. P.: A critical evaluation of a long pathlength cell for flow-based spectrophotometric measurements. Microchemical Journal 90, 19 (2008)

[IRV1970] Irving, H., Sinha, S. P.: Formation constants of europium(III)-salicylate complexes and their extraction into isoamyl alcohol. Anal. Chim. Acta. 49, 449 (1970)

[JOS2011] Joseph, C.: Sorption of uranium(VI) onto Opalinus Clay in the absence and presence of humic acid in Opalinus Clay pore water. Chem. Geol. 284, 240 (2011)

[JOS2011b] Joseph, C.: personal communication, Institute of Radiochemistry, Helmholtz Zentrum Dresden-Rossendorf, November 2011

[KIM1994] Kim, J. I., Klenze, R., Wimmer, H., Runde, W., Hauser, W.: A study of the carbonate complexation of Cm-III and Eu-III by time-resolved laser fluorescence spectroscopy. Journal of Alloys and Compounds 213, 333 (1994).

[KIM1994b] Kimura, T., Choppin, G. R.: Luminescence study on determination of the hydration number of Cm(III). J. Alloys Compd. 213, 313 (1994)

[KIM1998] Kimura, T., Kato, Y.: Luminescence study on determination of the inner-sphere hydration number of Am(III) and Nd(III). J. Alloys Compd. 271, 867 (1998)

[KIM2001] Kimura, T., Nagaishi, R., Kato, Y., Yoshida, Z.: Luminescence study on solvation of americium(III), curium(III) and several lanthanide(III) ions in nonaqueous and binary mixed solvents. Radiochim. Acta. 89, 125 (2001)

[KLI2007] Klimach, T., Amayri, S., Reich, T.: Sorption isotherms for ^{241}Am(III) on kaolinite. Jahresberichte, Institut für Kernchemie, Universität Mainz (2007)

[KRE2007] Krepelova, A.: Influence of Humic Acid on the Sorption of Uranium(VI) and Americium(III) onto Kaolinit, Dissertation, Technische Universität Dresden, Fakultät Mathematik und Naturwissenschaften (2007)

[KRI1980] Krishnan, R., Binkley, J. S., Seeger, R., Pople, J. A.: Self-consistent molecular-orbital methods .20. Basis set for correlated wave-functions. J. Chem. Phys. 72, 650 (1980)

[KUB1999] Kubicki, J. D., Schroeter, L. M., Itoh, M. J., Nguyen, B. N., Apitz, S. E.: Attenuated total reflectance Fourier-transform infrared spectroscopy of carboxylic acids adsorbed onto mineral surfaces. Geochim. Cosmochim. Acta 63, 2709 (1999)

[KUK2010] Kuke, S., Marmodee, B., Eidner, S., Schilde, U., Kumke, M. U.: Intramolecular deactivation processes in complexes of salicylic acid or glycolic acid with Eu(III). Spectrochim. Acta A: Mol. Biomol. Spectrosc. 75, 1333 (2010)

[KUL1986] Kulshrestha, R., Sengar, N., Singh, M.: Polarograohic studies of mixed ligand complexes of europium(III) with α-, β- and γ-picolines & carboxylate ions. Indian J. of Chemistry 26A, 940 (1987)

[LAC2003] Lackovic, K., Johnson, B. B., Angove, M. J., Wells, J. D.: Modeling the adsorption of citric acid onto Muloorina illite and related clay minerals. J. Colloid Interface Sci. 267, 49 (2003)

[LAU2000] Lauber, M., Baeyens, B., Bradbury, M. H.: Physico-Chemical Characterisation and Sorption Measurements of Cs, Sr, Ni, Eu, Th, Sn and Se on Opalinus Clay from Mont Terri. Technischer Bericht NTB 00-11, NAGRA Nationale Genossenschaft für die Lagerung radioaktiver Abfälle (2000)

[LIM2010] Lim, L. H. V., Prebil, A. B., Ellmerer, A. E., Randolf, B. R., Rode, B. M.: Temperature Dependence of Structure and Dynamics of the Hydrated Ca(2+) Ion According to ab initio Quantum Mechanical Charge Field and Classical Molecular Dynamics. Journal of Computational Chemistry 31, 1195 (2010)

[LIN2005] Lindqvist-Reis, P., Klenze, R., Schubert, G., Fanghanel, T.: Hydration of Cm3+ in aqueous solution from 20 to 200 degrees C. A time-resolved laser fluorescence spectroscopy study. Journal of Physical Chemistry B 109, 3077 (2005)

[LUN1984] Lundqvist, R., Lu, J. F., Svantesson, I.: Hydrophilic complexes of the actinides. III. Lactates of Am^{3+}, Eu^{3+}, U^{4+} and UO_2^{2+}. Acta Chem. Scand. A. 38, 501 (1984)

[MAT2007] Mathur, J. N., Cernochova, K., Choppin, G. R.: Thermodynamics and laser luminescence spectroscopy of binary and ternary complexation of Am^{3+}, Cm^{3+} and Eu^{3+} with citric acid, and citric acid + EDTA at high ionic strength. Inorg. Chim. Acta 360, 1785 (2007)

[MIC2003] Michel, U., Resnick, P., Kipp, B., DeSimone, J. M.: Copolymerization of tetrafluoroethylene and 2,2-bis(trifluoromethyl)-4,5-difluoro-1,3-dioxole in supercritical carbon dioxide. Macromolecules 36, 7107 (2003)

[MOL2008] Moll, H., Johnsson, A., Schäfer, M., Pedersen, K., Budzikiewicz, H., Bernhard, G.: Curium(III) complexation with pyoverdins secreted by a groundwater strain of Pseudomonas fluorescens. BioMetals. 21, 219 (2008)

[MOM2005] Mompean F. J. (ed.): CHEMICAL THERMODYNAMICS OF COMPOUNDS AND COMPLEXES OF U, Np, Pu, Am, Tc, Se, Ni AND Zr WITH SELECTED ORGANIC LIGANDS, (Chemical Thermodynamics Vol. 9) Elesevier 2005

[MOU1999] Moulin, C., Wei, J., Van Iseghem, P., Laszak, I., Plancque, G., Moulin, V.: Europium complexes investigations in natural waters by time-resolved laser-induced fluorescence. Anal. Chim. Acta 396, 253 (1999).

[MÜL2010] Müller, M., Acker, M., Taut, S., Bernhard, G.: Complex formation of trivalent americium with salicylic acid at very low concentrations. J. Radioanal. Nucl. Chem. 286, 175 (2010)

[MUR1992] Murphy, E. M., Zachara, J. M., Smith, S. C., Phillips, J. L.: The sorption of humic acids to mineral surfaces and their role in contaminant binding. Sci. Tot. Environ. 118, 413 (1992)

[NAG2002] NAGRA: Projekt Opalinuston - Synthese der geowissenschaftlichen Untersuchungsergebnisse, Entsorgungsnachweis für abgebrannte Brennelemente, verglaste hochradioaktive sowie langlebige mittelaktive Abfälle. Technischer Bericht NTB 02-03, NAGRA National Cooperative for the Disposal of Radioactive Waste (2002)

[NEL2008] Neles, J., Mohr, S., Schmidt, G.: Endlagerung wärmeentwickelnder radioaktiver Abfälle in Deutschland; Anhang Abfälle Entstehung, Mengen und Eigenschaften von wärmeentwickelnden radioaktiven Abfällen. GRS Gesellschaft für Anlagen- und Reaktorsicherheit (2008).

[OHY1971] Ohyoshi, E., Ohyoshi, A.: A study of complexes with a polybasic acid - Am(III) Citrate complexes. J. Inorg. Chem. 33, 4265 (1971)

[PAT2007] Pathak, P. N., Choppin, G. R.: Effect of complexing anions on europium sorption on suspended silica: a TRLFS study for ternary complex formation. Radiochim. Acta 95, 267 (2007)

[PLA2003] Plancque, G., Moulin, V., Toulhoat, P. and Moulin, C.: Europium speciation by time-resolved laser-induced fluorescence. Anal. Chim. Acta 478, 11 (2003)

[POW2005] Powell, K. J.: The IUPAC Stability Constants Database. (2005).

[PUR1972] Purdie, N., Tomson, M. B., Riemann, N.: The Thermodynamics of Ionization of Polycarboxylic Acids. J. Solution Chem. 1, 465 (1972)

[RAB2000] Rabung, T., Stumpf, T., Geckeis, H., Klenze, R., Kim, J. I.: Sorption of Am(III) and Eu(III) onto gamma-alumina: experiment and modelling. Radiochim. Acta 88, 711 (2000)

[RAB2005] Rabung, T., Pierret, M.C., Bauer, A., Geckeis, H., Bradbury, M. H., Baeyens, B.: Sorption of Eu(III)/Cm(III) on Ca-montmorillonite and Na-illite. Part 1: Batch sorption and time-resolved laser fluorescence spectroscopy experiments, Geochimica et Cosmochimica Acta, 69 5393 (2005)

[RAO1987] Rao, V. K., Mahajan, G. R., Natarajan, P. R.: Hydrolysis and Carboxylate Complexation of Trivalent Americium. Inorg. Chim. Acta 128, 131 (1987)

[RAO2005] Rao, L., Zanonato, P. L., Di Bernardo, P.: Interaction of Actinides with Carboxylates in Solution: Complexation of U(VI), Th(IV), and Nd(III) with Acetate at Variable Temperatures. J. Nucl. Radiochem. Sci. 6, 31 (2005)

[RAO2010] Rao, L., Tian, G. Srinivasan, G. T., Zanonato, P. L., Di Bernardo, P.: Spectrophotometric and Calorimetric Studies of Np(V) Complexation with Acetate at Various Temperatures from T = 283 to 343 K. J. of Solution Chemistry, DOI 10.1007/s10953-010-9592-z (2010)

[RAR1985] Rard, J. A.: Chemistry and thermodynamics of europium and some of its simpler inorganic compounds and aqueous species. Chemical Review 85, 555 (1985)

[RES1997] Resnick, P. R., Buck, W. H. In *Modern Fluoropolymers* Scheirs, J., Ed. John Wiley & Sons: Chichester, 397 (1997)

[ROZ2009] Rozalen, M., Brady, P. V., Huertas, F. J.: Surface chemistry of K-montmorillonite: Ionic strength, temperature dependence and dissolution kinetics. J. Colloid Interface Sci. 333, 474 (2009)

[RUN2000] Runde, W., Van Pelt, C., Allen, P. G.: Spectroscopic characterization of trivalent f-elements (Eu, Am) solid carbonates. Journal of Alloys and Compounds 303, 182 (2000)

[SCH2008] Schott, J.: Temperaturabhängige Untersuchungen zur Komplexbildung von Eu(III) mit dem Huminstoff-Modellliganden 2,5-Dihydroxybenzoesäure. Bachelor thesis (2008)

[SCH2010] Schott, J., Acker, M., Barkleit, A., Taut, S., Bernhard, G.: Sorption of Eu(III) onto Opalinus Clay - temperature depending investigations. FZD-IRC Annual Report 2009, Forschungszentrum Dresden-Rossendorf (2010)

[SCH2010b] Schott, J.: Untersuchungen zum Einfluss der Temperatur und kleiner organischer Liganden auf die Sorption von Eu(III) am Opalinuston. Master thesis, TU Dresden (2010)

[SCH2011] Schott, J. Acker, M, Barkleit, A., Brendler, V., Taut, S., Bernhard, G.: The influence of temperature and small organic ligands on the sorption of Eu(III) on Opalinus Clay, Radiochimica Acta accepted (2011)

[STE2011] Steudtner, R., Müller, K., Schmeide, K., Sachs, S., Bernhard, G.: Binary and Ternary Uranium(VI) Humate Complexes Studied by Attenuated Total Reflection Fourier-transform Infrared Spectroscopy. Dalton Trans. (2011) submitted

[STU2002] Stumpf, T., Bauer, A., Coppin, F., Fanghänel, T., Kim, J. I.: Inner-sphere, outer-sphere and ternary surface complexes: a TRLFS study of the sorption process of Eu(III) onto smectite and kaolinite. Radiochim. Acta 90, 345 (2002)

[STU2006] Stumpf, T., Fernandes, M. M., Walther, C., Dardenne, K., Fanghänel, T.: Structural characterization of Am incorporated into calcite: A TRLFS and EXAFS study. J. Colloid Interface Sci. 302, 240 (2006)

[TAK1998] Takahashi, Y., Minai, Y., Kimura, T., Tominaga, T.: Adsorption of europium(III) and americium(III) on kaolinite and montmorillonite in the presence of humic acid. J. Radioanal. Nucl. Chem. 234, 277 (1998)

[TER2005] Tertre, E., Berger, G., Castet, S., Loubet, M., Giffaut, E.: Experimental sorption of Ni^{2+}, Cs^{+} and Ln^{3+} onto a montmorillonite up to 150°C. Geochim. Cosmochim. Acta 69, 4937 (2005)

[TER2006] Tertre, E., Berger, G., Simoni, E., Castet, S., Giffaut, E., Loubet, M., Catalette, H.: Europium retention onto clay minerals from 25 to 150°C: Experimental measurements, spectroscopic features and sorption modelling. Geochim. Cosmochim. Acta 70, 4563 (2006)

[TER2006b] 45. Tertre, E., Castet, S., Berger, G., Loubet, M., Giffaut, E.: Surface chemistry of kaolinite and Na-montmorillonite in aqueous electrolyte solutions at 25 and 60 °C: Experimental and modeling study. Geochim. Cosmochim. Acta 70, 4579 (2006).

[THO1993] Thouvenot, P., Hubert, S., Moulin, C., Decambox, P., Mauchien, P.: Americium trace determination in aqueous and solid matrices by time-resolved laser-induced fluorescence. Radiochim. Acta. 61, 15 (1993)

[TIA2010] Tian, G. X., Martin, L. R., Rao, L. F.: Complexation of Lactate with Neodymium(III) and Europium(III) at Variable Temperatures: Studies by Potentiometry, Microcalorimetry, Optical Absorption, and Luminescence. Inorg. Chem. 49, 10598 (2010)

[TOR2005] Toraishi, T., Nagasaki, S., Tanaka, S.: A theoretical study on molecular structure of Eu(III)-salicylate complexes in aqueous system. Theochem-J. Mol. Struct. 757, 87 (2005)

[VAN2003] Van Loon, L. R., Soler, J. M., Bradbury, M. H.: Diffusion of HTO, $^{36}Cl^{-}$ and $^{125}I^{-}$ in Opalinus Clay samples from Mont Terri: Effect of confining pressure. J. Contam. Hydrol. 61, 73 (2003)

[WAN1999] Wang, Z. M., van de Burgt, L. J., Choppin, G. R.: Spectroscopic study of lanthanide(III) complexes with carboxylic acids. Inorg. Chim. Acta. 293, 167 (1999)

[WAN2004] Wang, X. K., Rabung, T., Geckeis, H., Panak, P. J., Klenze, R., Fanghänel, T.: Effect of humic acid on the sorption of Cm(III) onto gamma-Al_2O_3 studied by the time-resolved laser fluorescence spectroscopy. Radiochim. Acta 92, 691 (2004)

[WAT1997] Waterbury, R. D., Yao, W., Byrne, R. H.: Long pathlength absorbance spectroscopy: trace anaylsis of Fe(II) using a 4.5 m liquid core waveguide. Anal. Chim. Acta 357, 99 (1997)

[WIL2005] Wilson, R. E., Hu, Y.-J., Nitsche, H.: Detection and quantification of Pu(III, IV, V, and VI) using a 1.0-meter core waveguide. Radiochim. Acta 93, 203 (2005)

[WOL1992] Wolery, T. J.: EQ3/6, A Software Package for the Geochemical Modeling of Aqueous Systems. UCRL-MA-110662 Part I. Lawrence Livermore National Laboratory (1992).

[WU2009] Wu, T., Amayri, S., Drebert, J., Van Loon, L. R., Reich, T. : Neptunium(V) Sorption and Diffusion in Opalinus Clay. Environ. Sci. Technol. 43, 6567 (2009).

[YUS1990] Yusov, A. B.: Photoluminescence of americium(III) in aqueous and organic solutions. J. Radioanal. Nucl. Chem. 143, 287 (1990)

[ZAN2001] Zanonato, P. L., Di Bernardo, P., Bismondo, A., Rao, L., Choppin, G. R.: Thermodynamic studies of the complexation between Neodymium and Acetate at Elevated Temperatures. J. Solution Chem. 30, 1 (2001)

[ZES2011] Zessin, J.: UV/VIS-Spektroskopische Untersuchungen zur Komplexierung von Neodym(III) mit Pyromellitsäure. Bachelor thesis, TU Dresden (2011)

[ZOT2002] Zotov, A. V., Tagirov, B. R., Diakonov, I. I., Ragnarsdottir, K. V.: A potentiometric study of Eu^{3+} complexation with acetate ligand from 25 to 170°C at P_{sat}. Geochim. Cosmochim. Acta 66, 3599 (2002)

Berichtsblatt

1. ISBN oder ISSN geplant	2. Berichtsart (Schlussbericht oder Veröffentlichung) Schlussbericht

3. Titel

Verbundvorhaben: Wechselwirkung und Transport von Actiniden im natürlichen Tongestein unter Berücksichtigung von Huminstoffen und Tonorganika
Teilprojekt: Untersuchungen zur Temperaturabhängigkeit der Komplexbildung und Sorption dreiwertiger Actinide (Am(III), Pu(III)) im System Actinid-NOM-natürliches Tongestein-Aquifer

4. Autor(en) [Name(n), Vorname(n)]

Acker, Margret
Barkleit, Astrid
Müller, Melanie
Schott, Juliane
Bernhard, Gert

5. Abschlussdatum des Vorhabens
30.06.2011

6. Veröffentlichungsdatum
geplant

7. Form der Publikation
Karlsruher Institut of Technologie, wissenschaftliche Berichte

8. Durchführende Institution(en) (Name, Adresse)
1) TU Dresden
Fakultät für Mathematik und Naturwissenschaften
Institut für Analytische Chemie
01062 Dresden
2) TU Dresden
Sachgebiet Strahlenschutz
01062 Dresden

9. Ber. Nr. Durchführende Institution

10. Förderkennzeichen
FKZ: 02E10417

11. Seitenzahl
57

12. Fördernde Institution (Name, Adresse)

Bundesministerium für
Wirtschaft und Technologie (BMWi)
011019 Berlin

13. Literaturangaben
109

14. Tabellen
21

15. Abbildungen
25

16. Zusätzliche Angaben

17. Vorgelegt bei (Titel, Ort, Datum)

18. Kurzfassung
Zur Risikoabschätzung einer möglichen Actinidenmigration im Falle eines nichtbestimmungsgemäßen Betriebs eines Endlagers für hoch- und mittelradioaktive Abfälle sind thermodynamische Daten für eine reale Beschreibung der Wechselwirkung der Actinide mit der geologischen Barriere (Wirtsgestein) und den gelösten und suspendierten Bestanteilen im Aquifer (Wasserpfad) unerlässlich. Bisher nur unvollständig beantwortet ist Fragestellung zum Einfluss höherer Temperaturen auf die Migration der Actinide in natürlichen Tonbarrieren. Die thermodynamischen Datenbanken weisen hinsichtlich Daten für höhere Temperaturen erhebliche Lücken auf. Ziel des Projektes war es, thermodynamische Daten aus temperaturabhängigen Untersuchungen zur Komplexierung und Sorption von Am(III) im System An(III)-natürliches Tongestein-natürliche organische Materie zu gewinnen und damit die thermodynamische Datenbasis zu verbessern. Ein Schwerpunkt des Projektes lag auf temperaturabhängigen fluoreszenz- und absorptionsspektroskopischen Untersuchungen zur Charakterisierung der Wechselwirkung von Am(III) mit kleinen organischen Liganden (Pyromellitsäure, Salicylsäure, Milchsäure, Essigsäure, Zitronensäure und Weinsäure), die als Modellliganden für Huminstoffe und lösliche Tonorganika (natürliche organische Materie) fungieren. Verschiedene Eu(III)/Am(III)-Ligandkomplexe wurden spektroskopisch und thermodynamisch (logβ, ΔH, ΔS) charakterisiert, so. u.a. erstmalig Am(III)pyromellitsäure- und Am(III)salicylsäurekomplexe. Der zweite Schwerpunkt befasste sich mit der temperaturabhängigen Eu(III)sorption an dem natürlichen Tongestein Opalinuston unter Tonporenwasserbedingungen (pH = 7,6, I = 0,4 M) und in Anwesenheit von Zitronen- und Weinsäure. Die Eu(III)-Rückhaltung ist durch eine sehr starke Sorption am Ton (> 95%) gekennzeichnet, die generell mit steigender Temperatur zunimmt (Δ_sH ~50 kJ·mol^{-1}). In Gegenwart der Liganden sinkt die Eu(III)-Sorption ab, da diese Liganden mit dem Eu(III) im Porenwasser Komplexe bilden. TRLFS-Untersuchungen belegen, dass Eu(III)-Sorptionsspezies durch die Anwesenheit dieser organischer Liganden nicht verändert wird.
Die erzielten Ergebnisse tragen zu einer verbesserten, realitätsnäheren Beschreibung der Komplexierung und Sorption dreiwertiger Actinide in einem natürlichen Tongestein unter Endlagerbedingungen bei. Sie können in vergleichende Betrachtungen und Untersuchungen weiterer Wirtsgesteine (u.a. Salzstock mit Tonabdeckung, Tongesteine aus anderen Tonformationen) einbezogen und übertragen werden.

19. Schlagwörter
UV-Vis-Spektroskopie, Langweg-Kapillarzelle, Komplexierung, Americium, kleine organische Liganden, Sorption, Tongestein, Opalinuston, Europium, Batchsorptionsexperimente, zeitaufgelöste laserinduzierte Fluoreszenzspektroskopie (TRLFS), temperaturabhängig

20. Verlag	21. Preis

Document Control Sheet

1. ISBN or ISSN to be slated	2. type of document (e.g. report, publication) Final report

3. title

Joint Project: Interaction and transport of actinides in natural clay rock with consideration of humic substances and clay organics

Subproject: Investigations of temperature dependence of complexation und sorption of trivalent actinides (Am(III)) in the system actinid-NOM-natural clay rock-aquifer

4. author(s) (family name, first name(s)) Acker, Margret Barkleit, Astrid Müller, Melanie Schott, Juliane Bernhard, Gert	5. end of project 30.06.2011 6. publication date to be slated 7. form of publication Karlruher Institute of Technology, scientific report
8. performing organization(s) (name, address) 1) TU Dresden Fakultät für Mathematik und Naturwissenschaften Institut für Analytische Chemie 01062 Dresden 2) TU Dresden Sachgebiet Strahlenschutz 01062 Dresden	9. originator's report no. 10. reference no. FKZ: 02E10417 11. no. of pages 57
12. sponsoring agency (name, address) Bundesministerium für Wirtschaft und Technologie (BMWi) 011019 Berlin	13. no. of references 109 14. no. of tables 21 15. no. of figures 25

16. supplementary notes

17. presented at (title, place, date)

18. abstract

To assess the long-term safety of nuclear waste repositories for high level radioactive waste a wide knowledge about the chemical and physical behaviour of radionuclides, particularly the actinides, is essential. In worst case scenarios like a water inleakage into the repository a multitude of reactions of the stored radionuclides with solved or suspended components as well as interactions with the host rocks and backfill materials have to be considered quantitatively. The current thermodynamic databases are lacking fundamental data for the complexation of trivalent americium with small ligands at elevated temperatures. The complexation of Am(III)/Eu(III) with small organic ligands (pyromellitic, salicylic, lactic, acetic, citric, and tartaric acid) that serve as model ligands for natural organic material, like humic substances or clay organic was investigated by temperature dependent UV-vis and time-resolved laser-induced fluorescence spectroscopy (TRLFS). Several Am(III)/Eu(III)-organic ligand complexes were spectroscopically and thermodynamically characterized, so for the first time Am(III)-salicylate and Am(III)-pyromellitate complexes. From the temperature dependent complexation constants the complexation enthalpies and entropies were derived.

The sorption of Eu(III) on Opalinus Clay was investigated in absence and presence of the small organic ligands citric and tartaric acid at different temperatures and under synthetic pore water conditions (I = 0.4 M, pH = 7.6) by batch experiments. The Eu(III) retardation is characterized by a strong Eu(III) sorption on the clay(>95%). It was found, that the Eu(III) sorption increases generally with temperature in a considerably endothermic reaction with an enthalpy of about $\Delta_s H$ ~50 kJ·mol^{-1}. In presence of tartrate or citrate the Eu(III) sorption decreases with increasing ligand concentration due to a complex formation of Eu(III) in solution. This complex formation was verified by TRLFS investigations. The Eu(III) surface species on Opalinus Clay is no influenced by the presence of the studied organic ligands.

The obtained results contribute significantly to a more detailed and more realistic modelling about the complexation and sorption behaviour of trivalent actinides in natural clay minerals under the conditions of nuclear waste repository. Furthermore, the results extent the present thermodynamic database so that different geological formations can be assessed with respect to the eligibility criteria for a nuclear repository.

19. keywords

UV-Vis-absorptionspectroscopy, americium, long path flow cell, complexation, small organic ligands, sorption, natural clay rock, Opalinus clay, batchsorption experiment, time-resolved laser-induced fluorescence spectroscopy (TRLFS), temperature-dependent

20. publisher	21. price